PHOTOPRODUCTION OF POSITIVE K MESONS IN HYDROGEN

Thesis by

Paul Leighton Donoho

In Partial Fulfillment of the Requirements

For the Degree of

Doctor of Philosophy

California Institute of Technology

Pasadena, California

1958

ACKNOWLEDGMENTS

Dr. Robert L. Walker supervised this work and provided the inspiration for the development of much of the experimental technique. His invaluable counsel and continued assistance during the course of the experiment cannot be sufficiently acknowledged.

The constant encouragement and countless helpful suggestions of Dr. Robert F. Bacher are deeply appreciated. Dr. R. F. Christy, Dr. A. B. Clegg, Dr. R. Gomez, Dr. J. M. Teem, Dr. A. V. Tollestrup, and other members of the staff of the Synchrotron Laboratory offered advice on numerous occasions.

Mr. James I. Vette was the source of many helpful suggestions. The assistance of Mr. Howard M. Brody and Mr. Franklin P. Dixon in taking data is greatly appreciated. Dr. Vincent Z. Peterson and Mr. Earle B. Emery are to be thanked for their work in maintaining the liquid hydrogen target.

The engineering staff and crew of the Synchrotron Laboratory provided necessary construction and maintenance of equipment essential to the success of this experiment. Particular thanks are due to Mr. Dan D. Sell and Mr. Larry Loucks.

The support of the General Electric Company in the form of a predoctoral fellowship held during the course of this experiment is greatly appreciated.

The partial financial support of the Atomic Energy Commission is gratefully acknowledged.

ABSTRACT

In the experiment described here K^+ mesons produced in a liquid hydrogen target by the 1100 Mev bremsstrahlung from the California Institute of Technology Synchrotron have been observed. It has been found that the K^+ mesons are produced in association with Λ^o hyperons, as required by the law of associated production, thus confirming the validity of this law in electromagnetic interactions. The K^+ mesons are momentum analyzed in a magnetic spectrometer and identified by their energy loss in three scintillation counters, the very large background due to pions and protons being virtually eliminated by means of a time-of-flight velocity measurement. The differential cross section for the reaction $\gamma + P \rightarrow K^+ + \Lambda^o$ has been measured at photon energies of 960 Mev, 1000 Mev, and 1060 Mev at various K^+ meson laboratory angles between 15 degrees and 45 degrees. This cross section shows little variation with photon energy between 960 Mev and 1060 Mev. There is a decrease in the cross section at backward center-of-momentum angles at both 1000 Mev and 1060 Mev. The magnitude of the $K - \Lambda$ coupling constant estimated from these measurements is smaller by a factor of about five than the pion-nucleon coupling constant, if the K^+ meson is assumed to be pseudoscalar.

TABLE OF CONTENTS

I. INTRODUCTION

Since the discovery of the K mesons and hyperons, the so-called "strange" particles, the desire to understand their role in nature has inspired quite extensive experimental investigation of their properties. The experiment to be described here concerns the production of these particles in high-energy photonuclear interactions. Although the "strange" particles are produced plentifully in high-energy pion-nucleon and nucleon-nucleon collisions, they had not been observed prior to this experiment as products of photon-nucleon collisions. When the 1100 Mev bremsstrahlung beam of the electron synchrotron at the California Institute of Technology became available, this experiment was begun as an exploratory search for photoproduced K^+ mesons. It was desired to ascertain, firstly, whether they are produced at all, and, secondly, if they are, whether they are produced in association with another "strange" particle as required by the law of associated production of "strange" particles (1). It was found that K^+ mesons are produced in association with Λ^o hyperons when liquid hydrogen is bombarded by photons, and the cross section for this reaction has been measured at several energies and angles.

Because the law of associated production of "strange" particles, which is a consequence of the "strangeness" theory of Gell-Mann (2) and Nishijima (3), has been so successful in predicting which reactions are allowed among strongly interacting particles and because this law should be valid for the electromagnetic interactions also, if the principle of minimal electromagnetic interaction is correct (4), it was expected that K^+ mesons would be produced in association with at least one other "strange" particle, if at all. The only reactions which are

energetically possible at photon energies below 1100 Mev and which satisfy the requirements of the "strangeness" theory, namely that the "strangeness" quantum number be conserved in the interaction, are the following:

$$\gamma + P \rightarrow K^+ + \Lambda^o \quad (1)$$

$$\gamma + P \rightarrow K^+ + \Sigma^o \quad (2)$$

The threshold photon energies for these reactions are, respectively, 910 Mev and 1040 Mev. The law of associated production definitely forbids the reaction:

$$\gamma + P \rightarrow K^+ + N \quad (3)$$

This reaction, which becomes energetically possible at a photon energy of 630 Mev, would, if allowed, compete strongly with reactions 1 and 2. Since a determination of the occurrence or non-occurrence of this reaction provides a test of the validity of the "strangeness" theory for electromagnetic interactions, an attempt was made to determine the yield of K^+ mesons from reaction 3 alone. It was not, however, possible to identify any of the observed K^+ mesons as coming from this reaction; indeed, an upper limit of 5 per cent relative to reaction 1 can be assigned to the cross section for reaction 3.

In this experiment K^+ mesons having a desired momentum were selected by a magnetic spectrometer and identified by their energy loss in three scintillators placed at the spectrometer focus. An enormous background due to pions and protons was virtually eliminated by means of a time-of-flight measurement which permitted selection of only those

particles focused by the spectrometer which have the correct velocity for K^+ mesons of the required momentum. Because of the good resolution of the magnetic spectrometer it was possible to count only K^+ mesons from reaction 1, as explained in section II. Consequently, the differential cross section for this reaction was calculated from the measured K^+ mesons yields. The differential cross section was thus obtained for laboratory photon energies of 960 Mev, 1000 Mev, and 1060 Mev at various K^+ meson laboratory angles between 15 degrees and 45 degrees.

Because of the enormous amount of work which has gone into the investigation of K mesons and hyperons, many of their intrinsic properties, such as mass and lifetime, are well-established. The most recent determinations of these quantities (5) are listed in Table 1. These are the values adopted, where necessary, for the calculations of this experiment. Information pertaining to the interaction properties of these particles, such as spin, parity, and coupling strength, is rather limited, but these are the properties essential to a determination of the part played by these particles in the strong interactions. Consequently, the behavior of the K mesons and hyperons in nuclear production and scattering processes has recently received the bulk of experimental attention.

Several groups have studied "strange" particle production in pion-nucleon collisions at pion energies between 0.87 Bev and 1.3 Bev using propane bubble chambers (6). Proton-proton collisions at 3 Bev energy have been studied by groups using a hydrogen diffusion cloud chamber (7) and by groups using a liquid hydrogen target and counters (8).

Table I. Properties of K Mesons and Hyperons

Particle	Mass Mev.	Charge Electronic Units	Lifetime Seconds	T	S
K^+	494 ± 0.1	+1	$(1.24 \pm 0.02)\times10^{-8}$	1/2	+1
K^o	493 ± 5	0	K_1^0: $(0.95 \pm 0.08)\times10^{-10}$	1/2	+1
$\overline{K}^o$	493 ± 5	0	K_2^0: $(0.3 < \tau < 10)\times10^{-7}$	1/2	-1
K^-	494 ± 0.1	-1	$(1.24 \pm 0.02)\times10^{-8}$	1/2	-1
Λ^o	1114.8 ± 0.2	0	$(2.8 \pm 0.2)\times10^{-10}$	0	-1
Σ^+	1189.7 ± 0.2	+1	$(0.7 \pm 0.1)\times10^{-10}$	1	-1
Σ^o	1188.6^{+3}_{-2}	0	?	1	-1
Σ^-	1196.6 ± 0.4	-1	$(1.6 \pm 0.2)\times10^{-10}$	1	-1
Ξ^-	1321 ± 3.5	-1	$(4.6 < \tau < 200)\times10^{-10}$	1/2	-2

The results obtained from the study of both these interactions are limited so far, but they indicate somewhat weaker coupling of K mesons to baryons than the coupling of pions to nucleons. These results and their relationship to this experiment are discussed in section VII.

The scattering of K^+ mesons has been studied extensively in nuclear emulsions (9) and, to a lesser extent, in a liquid hydrogen bubble chamber (10). It has been found that the total cross section in emulsion nuclei is only one-fourth the usual geometric cross section. This fact is used in the calculation of the nuclear absorption correction necessary to this experiment. In addition, evidence is obtained from these scattering measurements which implies, as explained in section VII, that the K^+ meson is pseudoscalar like the pion, but coupled less strongly than the pion to baryons.

Other experiments for the purpose of studying K^+ meson photoproduction have been started and have produced preliminary results. Peterson, Roos, and Terman (11), using nuclear emulsions to detect K^+ mesons from a liquid hydrogen target, find a differential cross section based, so far, on six K^+ mesons detected which is in agreement with the results of this experiment. Ernstene, Gomez, Myers, and Tollestrup (12), using a counter telescope with side counters to detect the decay products of the K^+ mesons after they stop in the telescope, also have obtained preliminary results in rough agreement with those of this experiment. Wilson and Silverman (13), have used a counter telescope in connection with a magnetic spectrometer and side counters to detect the K^+ mesons from a liquid hydrogen target. Although the angle and energy of the K^+ mesons which they observe are quite different

from those of this experiment, their results are in qualitative agreement with those presented here. All the results obtained by these groups are discussed further and compared to the results of this experiment in section VIII.

Because the method developed during this experiment for the reliable detection of a low-yield particle like the K^+ meson may be useful in future experiments, it is described in detail in sections II through VI. In section VII theories having a bearing on the "strange" particle photoproduction process are described, and a comparison of their predictions to the results of this experiment is made in section VIII, which also contains a comparison of the results of this experiment to those obtained from the other experiments mentioned above.

II. EXPERIMENTAL TECHNIQUE

The identification of K^+ mesons in the presence of an extremely large background due to pions and protons is the principal problem encountered in this experiment. Once the K^+ mesons have been identified, however, there is the additional problem of the determination of the reaction in which they are produced. This section concerns the general methods used in the solution of these problems. Detailed descriptions of equipment, operating procedure, and data analysis appear in succeeding sections.

A preliminary attempt to detect photoproduced K^+ mesons was made shortly after the 1100 Mev bremsstrahlung beam of the electron synchrotron became available, a polyethylene target being used until the liquid hydrogen target was completed. Positively charged particles originating in the target having momentum of approximately 425 Mev at a laboratory angle of 35 degrees with respect to the bremsstrahlung beam, were focused at the center of three scintillation counters by the magnetic spectrometer described in section III. For K^+ mesons produced in association with Λ^o hyperons, photons of 1060 Mev energy are required. For singly produced positive pions at this momentum and angle, photons of 470 Mev/c are required, whereas, for recoil protons from single neutral pion production, 360 Mev photons are needed. Since the last two energies are fairly close to the 3/2-3/2 resonance in pion photoproduction, and the 1060 Mev required for K^+ meson production in the reaction assumed is not far from the 910 Mev threshold for this reaction, the ratio of the numbers of protons or pions to K^+ mesons was, a priori, expected to be quite large.

Figure 1 shows a typical pulse height spectrum obtained from the scintillation counter, C-2, placed at the spectrometer focus. Protons were stopped in an absorber placed before the counter so that only pions, electrons, and K mesons could, presumably, be counted. The spectrum shown exhibits a pion peak having almost precisely the spread predicted from fluctuations in the energy loss according to the theory of Symon (14). The solid curve superimposed on the experimentally obtained histogram is the distribution predicted by this theory. The observed position of the most probable pion pulse height was used to calculate the position of the most probable K^+ meson pulse height, which is indicated in the figure. There is, of course, no indication of a K^+ meson peak in this spectrum; indeed, because of the heavy weighting of the pion statistical fluctuations toward large energy losses, about ten per cent as many K^+ mesons as pions would be needed in order to distinguish reliably a K^+ meson peak. Since this measurement showed that the yield of K^+ mesons is indeed quite small compared to that for the pions, a method of discrimination against the background independent of both the momentum and pulse-height requirements was sought.

R. L. Walker noticed that the path length between the foci of the magnetic spectrometer, about 4 meters, is sufficient to make a time-of-flight velocity measurement permitting discrimination against particles of the same momentum as the K^+ mesons but having different masses. Figure 2 shows the time of flight between foci for K^+ mesons, pions, and protons. At the highest momentum considered, about 520 Mev/c, the separation in time of flight between K^+ mesons and pions is 4.2 millimicroseconds, the shortest separation encountered.

Figure 1. Pulse-Height Spectrum in C-2.

This figure illustrates the difficulty of identifying K mesons on the basis of pulse-height alone. The histogram is the measured spectrum of pions and K mesons, and the dashed curves give the spectrum predicted on the basis of Symon's theory of energy-loss fluctuations for both pions and K mesons.

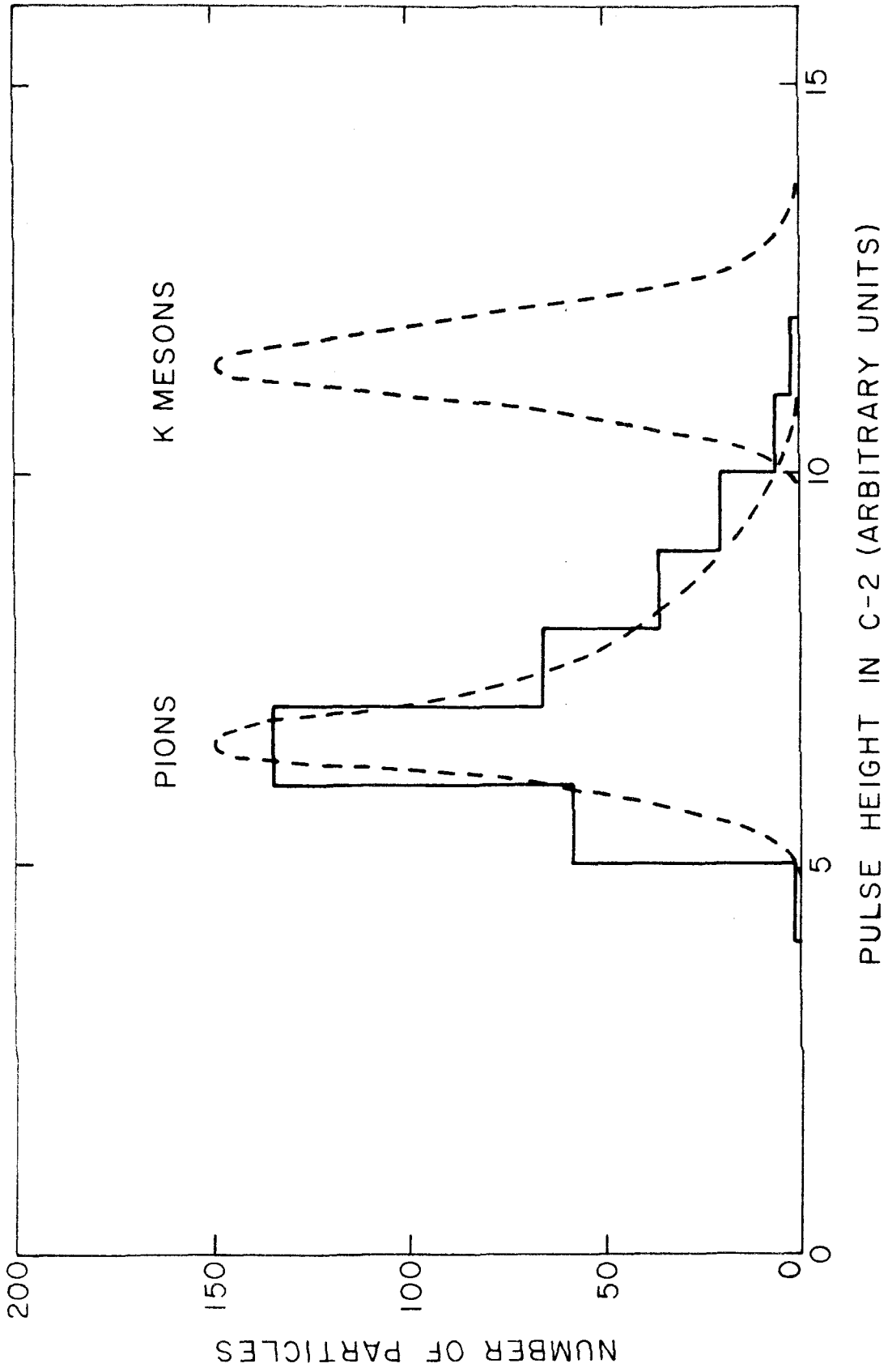
K MESONS
PIONS
NUMBER OF PARTICLES
0
50
100
150
200
0
5
10
15
PULSE HEIGHT IN C-2 (ARBITRARY UNITS)

Figure 2. Time of Flight Between Spectrometer Foci.

This figure shows the time of flight as a function of particle momentum for protons, pions, and K mesons.

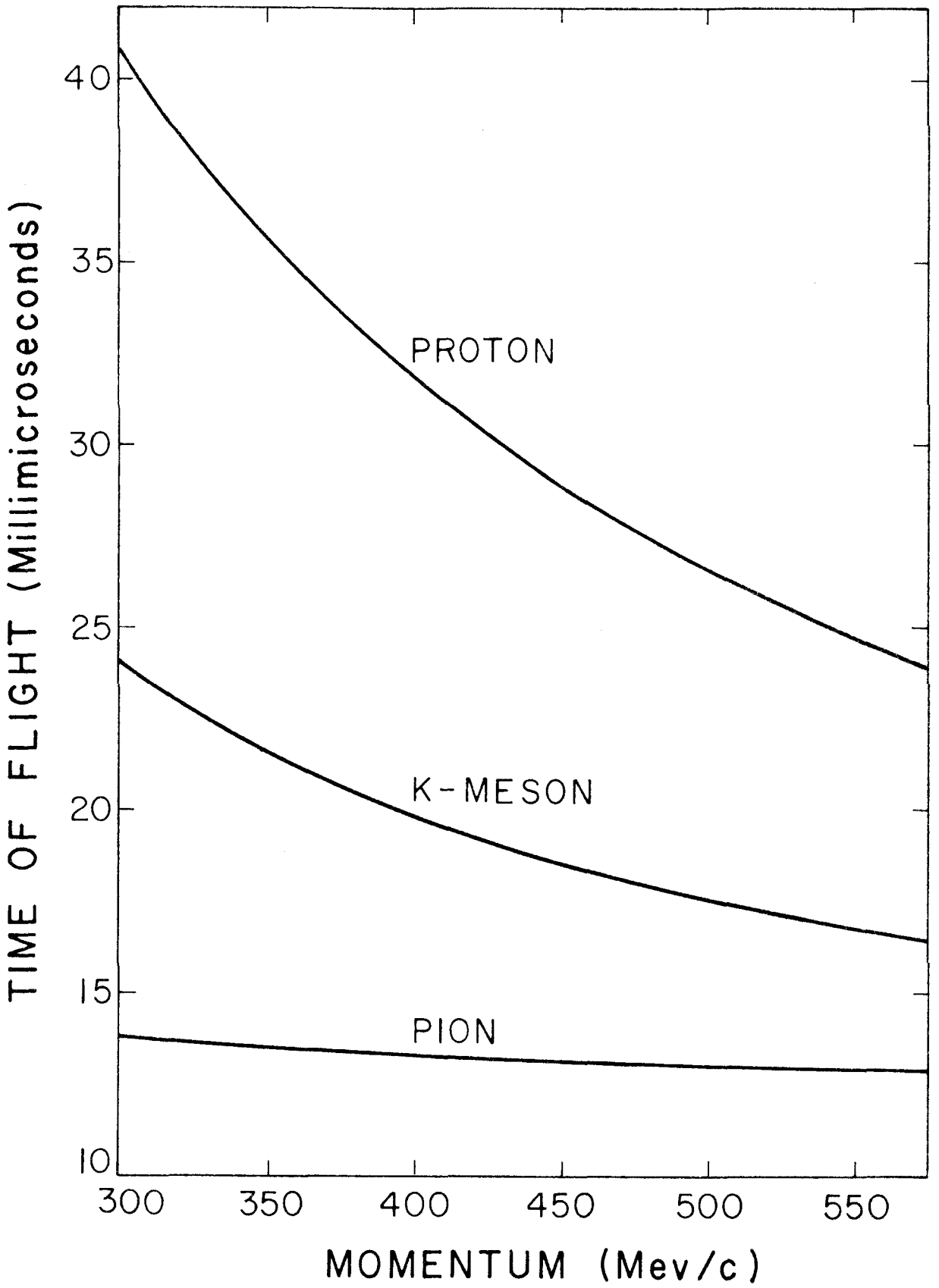
TIME OF FLIGHT (Millimicroseconds)
40
35
30
25
20
15
10
PROTON
K-MESON
PION
300
350
400
450
500
550
MOMENTUM (Mev/c)

Since resolution of time intervals this short is well within the capabilities of existing electronic techniques, it was possible to construct a system capable of detecting K^+ mesons with only 10 to 20 per cent background contamination.

A schematic representation of the system used is shown in Figure 3. The momentum interval accepted by the spectrometer is determined by the width of counter C-2, and the angular interval accepted is defined by a lead-lined aperture described in section III. The counter, C-0, initiates the time-of-flight measurement, and it is, therefore, placed as near the target as possible, the distance being determined by counting-rate limitations in this counter. A fast coincidence circuit is used to detect coincidences between signals from C-2 and suitably delayed signals from C-0, the delay being chosen such that coincidences occur for particles having the correct velocity for K^+ mesons of the required momentum. Because the counting rate in C-0 is very high (about 5×10^6 counts per second), the rate of accidental coincidences in the fast coincidence circuit is rather large. Since, however, a large fraction of the particles counted in C-2 is due to general laboratory background rather than to particles focused by the magnet, a considerable reduction in accidental counting is effected by requiring a "slow" (0.1 microsecond) coincidence between the output of the fast coincidence circuit and signals from counters C-1 and C-3. These additional counters, which are located such that they require particles to come from the direction of the spectrometer magnet when they are put into coincidence with C-2, provide useful pulse-height information as well as reduce the accidental rate greatly.

Figure 3. Experimental Arrangement

A cross-sectional view taken through the median plane of the magnetic spectrometer.

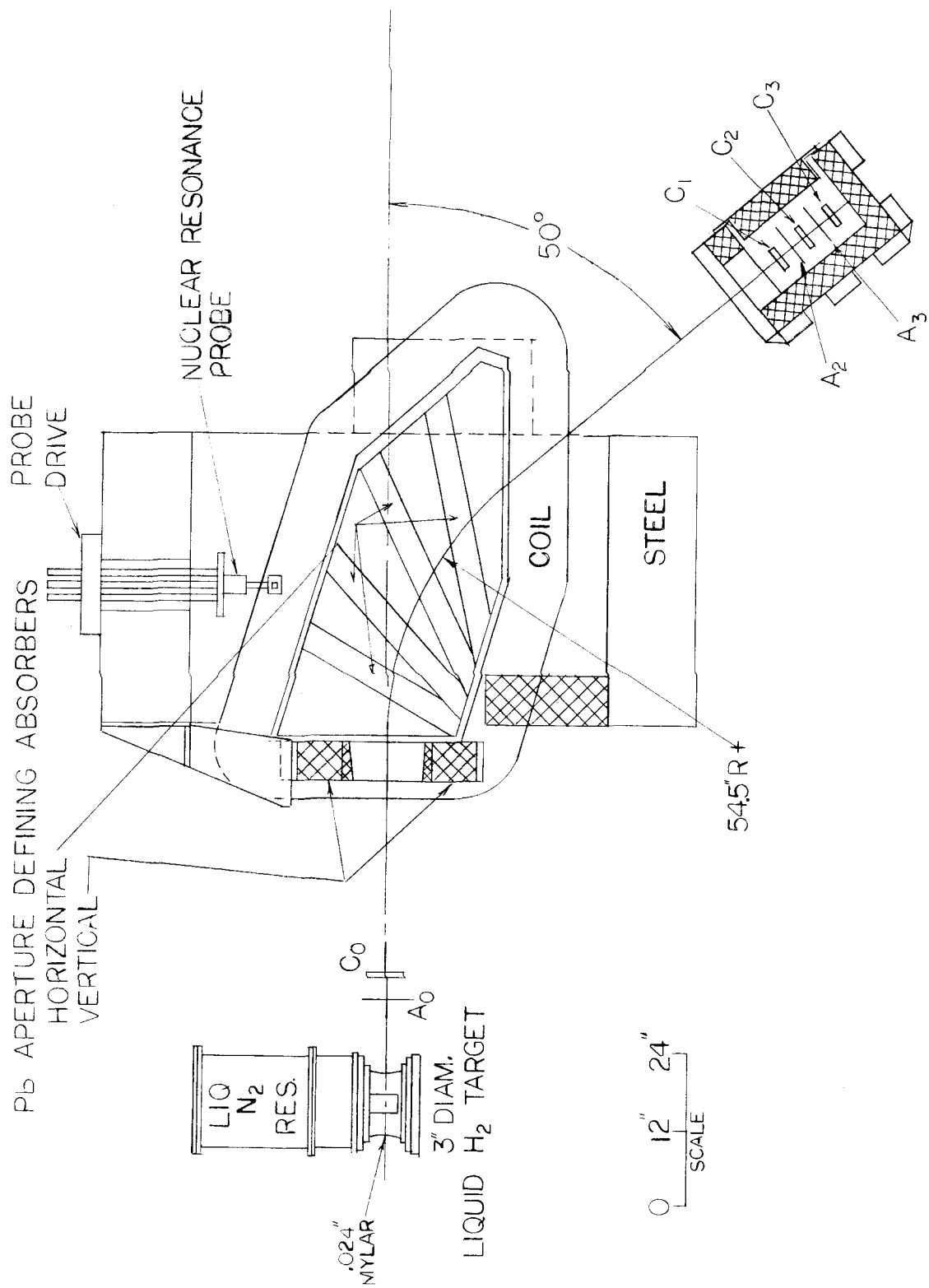
Pb APERTURE DEFINING ABSORBERS
HORIZONTAL
VERTICAL
PROBE DRIVE
NUCLEAR RESONANCE PROBE
COIL
STEEL
50°
54.5" R +
C_1
C_2
C_3
A_2
A_3
C_0
A_0
LIQ N_2 RES.
3" DIAM.
LIQUID H_2 TARGET
.024" MYLAR
0 12" 24"
SCALE

FIGURE 3

Accidental counting could not, however, be entirely eliminated by this means. In addition, the resolution of the fast coincidence circuit could not be made sharp enough to discriminate perfectly against pions at the higher momenta considered without losing K^+ mesons, as explained in section III. As a result, from ten to twenty pions were still counted for each K^+ meson counted. Pulse-height spectra in each of the counters were obtained, consequently, in which K^+-meson peaks could be seen but not clearly resolved. Fortunately, the K^+-meson yield was large enough that most of this background could be eliminated by correlating the pulse heights in the three counters, C-1, C-2, and C-3 for each particle counted. Then, since the fluctuations in energy loss for the pions are not correlated from one counter to another, the K^+ mesons can easily be distinguished from the pions. The actual technique of identifying the K^+ mesons is explained in detail in section V. The question of the remaining background is best left until a discussion of the reaction kinematics is given.

The three reactions energetically capable of producing K^+ mesons are given again here:

$$\gamma + P \rightarrow K^+ + \Lambda^o \qquad (1)$$

$$\gamma + P \rightarrow K^+ + \Sigma^o \qquad (2)$$

$$\gamma + P \rightarrow K^+ + N \qquad (3)$$

It must be remembered, of course, that reaction 3 is forbidden by the law of associated production and is being considered here only as

a possible test of this law. Because of the two-particle initial and final states of these reactions, a knowledge of the momentum and direction of one of the final-state particles is sufficient to determine uniquely the energy of the photon causing the reaction. Figure 4 shows the relation between K^+ meson laboratory momentum and angle at constant photon energy. Curves for several different photon energies for each of the above reactions are given. The shaded region shown in this figure depicts the sensitive region of the magnetic spectrometer when set to an angle of 25 degrees and a momentum of 425 Mev/c. For reaction 1 this point corresponds to a photon energy of 1000 Mev, whereas for reaction 2 a photon energy of 1130 Mev is needed. Since the bremsstrahlung used had an endpoint usually at 1100 Mev, reaction 2 did not contribute to the K^+ meson yield at this point. For measurements at 960 Mev, however, reaction 2 could contribute K^+ mesons if the bremsstrahlung endpoint were at 1100 Mev. The endpoint was, therefore, reduced to about 1080 Mev when counting K^+ mesons produced by 960 Mev photons. If reaction 3 occurs, however, it can contribute to the K^+-meson yield, since a photon energy of only 720 Mev is required. A means of detecting any contribution from this reaction is, fortunately, quite simple: the synchrotron energy is lowered until reaction 1 can no longer contribute to the K^+-meson counting rate. The yield from reaction 3 will not be changed and can, therefore, be measured.

This method of lowering the synchrotron energy to detect the background from reaction 3 was used also to determine the background from other sources. Since the liquid hydrogen target gives an extremely

Figure 4. Kinematics of K Meson Photoproduction

This figure gives K meson laboratory momentum as a function of laboratory angle at constant photon energy for reactions energetically capable of yielding K mesons.

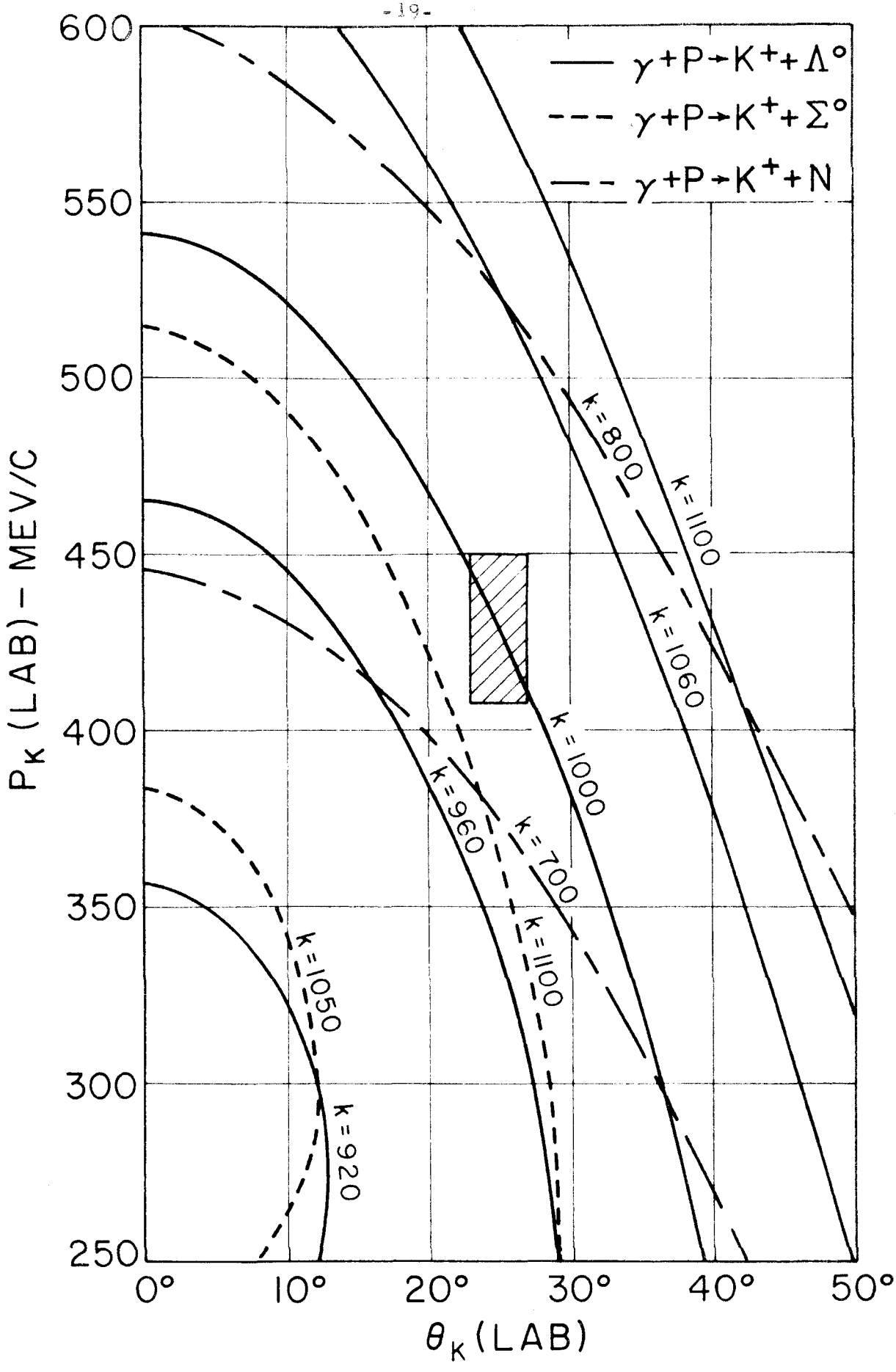
γ+P→K⁺+Λ°
γ+P→K⁺+Σ°
γ+P→K⁺+N
K=800
K=1100
K=1060
K=1000
K=960
K=700
K=1100
K=1050
K=920
600
550
500
450
400
350
300
250
0°
10°
20°
30°
40°
50°
P_K (LAB) – MEV/C
θ_K (LAB)

low counting rate due to non-hydrogen events (because of the good collimation achieved by requiring particles to pass through both C-0 and the spectrometer aperture), the sources of background seem to be the following:

(1) K^+ mesons from reaction 3;

(2) accidentally counted pions, as mentioned above;

(3) protons of momentum too high to be focused, which scatter from various parts of the spectrometer magnet in such a way that they arrive at counter C-2 with the right time of flight to be counted. These last two sources should not be changed appreciably by lowering the synchrotron energy, since only a small portion of the bremsstrahlung spectrum is thereby removed, and only the pions and protons of the highest energy are affected. Although there is no direct way to check this assumption, it is shown in section V that the assumption is certainly reasonable. Presumably, therefore, all background can be accounted for by means of one low-energy measurement at each experimental point. The backgrounds as measured in this way ranged between 5 and 25 per cent of the K^+ meson counting rates observed.

One last point which should be mentioned in this section concerns the decay in flight of the K^+ mesons. Because of the long path length which they must travel between the spectrometer foci their 12.4 millimicrosecond lifetime (5) causes the decay in flight of 65 to 85 per cent of the K^+ mesons which would otherwise be counted. This is a major difficulty in this experiment, but there is, of course, no way to eliminate it for this apparatus. Indeed, the long path length, which

necessitates the large decay correction, makes possible the time-of-flight measurement without which this experiment could not be performed.

III. EQUIPMENT

The Magnetic Spectrometer

A conventional single-focusing spectrometer capable of focusing charged particles of momenta as high as 600 Mev/c was used in this experiment. A more complete description of this instrument can be found elsewhere (15). A momentum dispersion $\Delta p/p_o = 0.0984$ and a solid angle $\Delta\Omega = 0.00748$ were obtained under the conditions of this experiment. The median angle of deflection in the magnetic field is 50 degrees, and the path length between foci is 165 inches. A cross sectional view of the spectrometer taken through its median plane is shown in figure 3.

The wedge-shaped uniform-field magnet is powered by a current-regulated motor-generator set. A magnetic field of approximately 15 kilogauss is obtained at 50-kilowatt input to the water-cooled coils of the magnet. The field is monitored at all times by a nuclear resonance magnetometer and can be maintained at any desired value within its range with a precision of 0.1 per cent. The vertically deflecting magnet, weighing approximately 40 tons, is mounted on wheels and pivoted about a vertical axis passing through the center of the liquid hydrogen target to facilitate angular positioning. Laboratory angles between 24 degrees and 156 degrees are readily accessible, with angles in the region from 0 degrees to 24 degrees being available if the bremsstrahlung beam of the synchrotron is allowed to strike the magnet framework.

The focusing properties of the spectrometer were investigated by means of the so-called floating-wire technique, which permits the tracing of actual orbits through the magnetic field (16). These measurements were made with care, resulting in probable errors on the measured quantities of one per cent or less (15).

Since the momentum dispersion is determined by the width of the counter, C-2, placed at the spectrometer focus, the measurements were made with a "dummy" counter of the size used in this experiment, but constructed so that the orbit of the wire could be traced through various points on the counter. The measurements determined the momentum which a particle would need in order to pass through specified points in the target, counter, and aperture. In this way a momentum response function for the spectrometer was obtained and is plotted in figure 5(a). This response function gives the relative response of the spectrometer to particles of different momenta and is normalized by the following expression:

$$\frac{\Delta p}{p_o} = \int_{p_{min}}^{p_{max}} g(p, p_o)dp \qquad (4)$$

The limits on the integral, p_{min} and p_{max} are the momenta between which the response function, $g(p, p_o)$, does not vanish. The quantity p_o is the central momentum in the interval of acceptance, and was measured as a function of the magnetic field. In figure 5(a) the response function is averaged over the three-inch hydrogen target. It is shown in section VI that this function, which gives the relative response of the

Figure 5. Magnetic Spectrometer Response.

(a) Relative response to particles as a function of momentum.

(b) Relative response to particles as a function of angle.

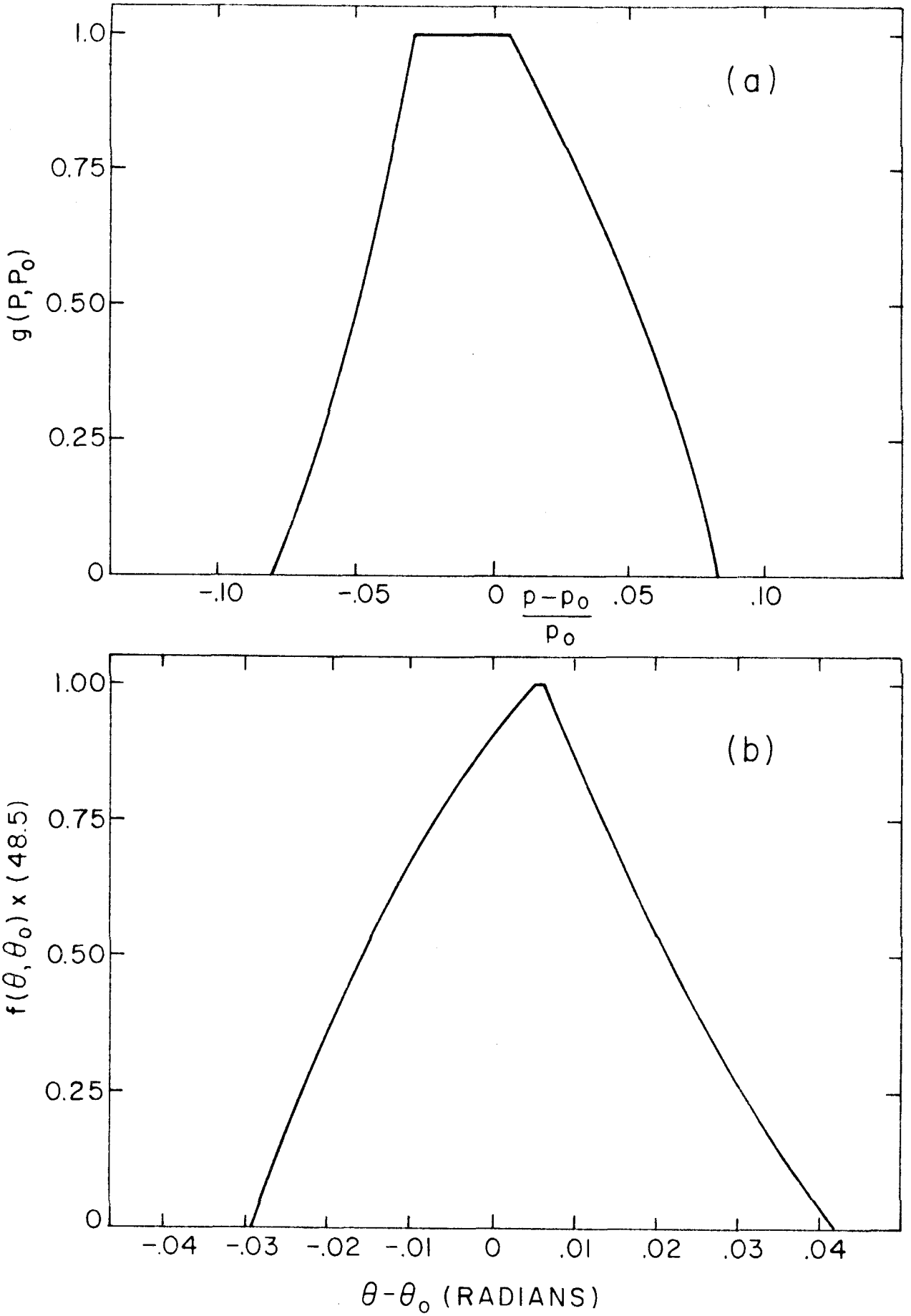
(a)
1.0
0.75
0.50
0.25
0
g(P,P0)
-.10
-.05
0
p−p0 / p0
.05
.10
(b)
1.00
0.75
0.50
0.25
0
f(θ,θ0) x (48.5)
-.04
-.03
-.02
-.01
0
.01
.02
.03
.04
θ-θ0 (RADIANS)

spectrometer to various momenta, is often useful in the interpretation of yields obtained with the spectrometer.

The aperture of the magnet, which defines the solid angle of acceptance of the spectrometer, is limited by four pairs of lead absorbers within the magnetic field, as shown in figure 3, which define the horizontal extent of the aperture. The vertical extent of the aperture is defined by two lead absorbers placed at the entrance to the field. Of the horizontal defining absorbers, only the pair farthest from the target limits the aperture, whereas the other three pairs serve only to prevent particles which scatter from the pole pieces of the magnet from entering the counters. All these lead absorbers are tapered to point toward the center of the target in order to minimize scattering and penetration.

Since the horizontal defining slit is inside the magnet and is not at a uniform distance from the target, the extent of the horizontal aperture was investigated also with the floating-wire technique. The limiting horizontal angular deflections were measured as a function of the vertical position in the aperture. In this way a detailed knowledge of the angular acceptance interval of the spectrometer was obtained. In figure 5(b) is plotted an angular response function for the spectrometer, which gives the relative response to particles of different angles and is normalized by the following expression:

$$\Delta\Omega = \int_{\theta_{min}}^{\theta_{max}} f(\theta, \theta_o)d\theta \qquad (5)$$

where θ_{min} and θ_{max} are the angular limits for a given setting of the spectrometer, θ_o, between which the response function $f(\theta, \theta_o)$ does not vanish. This function is averaged over the target volume in the figure. It is useful in the interpretation of the yield obtained with the spectrometer, as explained in section VI.

It was not possible to achieve double focusing with this spectrometer because of the long focal distance which would be required. There is actually considerable fringe-field defocusing. Consequently, the counters were made long enough that they collect all particles coming through the magnet (with the right momentum) without limiting the solid angle. The two counters, C-1 and C-3, are just large enough that they do not limit the momentum interval defined by C-2 if a 123 coincidence is required. Such a coincidence then reduces the background greatly without restricting the desired counting. The counters are shielded from general laboratory background by a steel box which supports a four-inch thickness of lead.

The Scintillation Counters

All counters used in this experiment were fabricated from a polystyrene-base plastic scintillator obtained from the University of California Radiation Laboratory at Livermore. The dimensions of the counters are as follows:

Counter	Dimensions
C-0	3.25" x 5" x 0.375"
C-1	5.75" x 11" x 0.78"
C-2	4.75" x 11" x 0.78"
C-3	5.75" x 11" x 0.39"

Because of the proximity of the spectrometer magnet all photomultipliers associated with these counters were magnetically shielded with two Mumetal shields and one soft-iron shield. As a result, there was little effect upon their gain except at the highest fields, where only one measurement was made.

Since the counter C-0 was subjected to an especially high counting rate because of its proximity to the hydrogen target, precautions were taken to insure its reliable operation. Especial care was exercised in the stabilization of the dynode potentials for the RCA Type 6810A photomultiplier: large capacitors were placed between the dynodes to supply the very large peak currents required. Consequently, little reduction in gain was observed, even at a counting rate of 5×10^6 particles per second. Unless an absorber was placed, however, between C-0 and the hydrogen target to stop the flood of very-low-energy particles from reaching this counter, reliable operation could not be obtained. Generally, at angles of 25 degrees or larger, 1/2 inch of polyethylene was used, but at the 15 degree point a 3-inch carbon absorber was required.

Because of the action of the magnet in filtering out all particles except for those in a 10 per cent momentum band, the counting rates in

C-1, C-2, and C-3 were all fairly low -- about 1 or 2 counts per millisecond. Since it was desired to identify particles on the basis of energy loss in these counters, an attempt was made to reduce statistical pulse-height fluctuations by collecting the light from the counters as efficiently as possible. Each of these counters was viewed, therefore, by two photomultipliers whose outputs were balanced to give the best possible resolution. All photomultipliers used were RCA Type 6655 except for one RCA Type 6810A which was associated with C-2 in order to provide large pulses for direct operation of the fast coincidence circuit described below.

Despite the attempt to improve resolution, the dispersion in the counters was rather large. This is, of course, due mainly to statistical fluctuations in the energy loss, which cannot be improved beyond the value predicted by Symon's theory of the fluctuations in the energy loss (14). A typical pulse height spectrum in C-1 is shown in figure 6. This spectrum includes both pions and protons at a momentum of 468 Mev/c. The actual spectrum obtained is plotted as a histogram, the curves being the distributions predicted by Symon's theory. Part of the broadening of the proton peak is due to the momentum spread of the particles making up the peak. For K^+ mesons, which were usually about two to three times minimum ionizing, the dispersion was considerably less than that of the pions, making their identification easier. Symon's prediction for the K meson distribution is also shown in figure 6. Although this distribution falls within the tail of the pion distribution, the correlation of the pulse heights in all three counters

Figure 6. Pulse-Height Spectrum in C-1

The histograms are the measured spectra of pions and protons at a momentum of 468 Mev/c. The dashed curves give the dispersion predicted by Symon's theory of the energy-loss fluctuations for protons, pions, and K mesons. The curves for the protons and the K mesons include the dispersion due to the momentum spread accepted by the spectrometer.

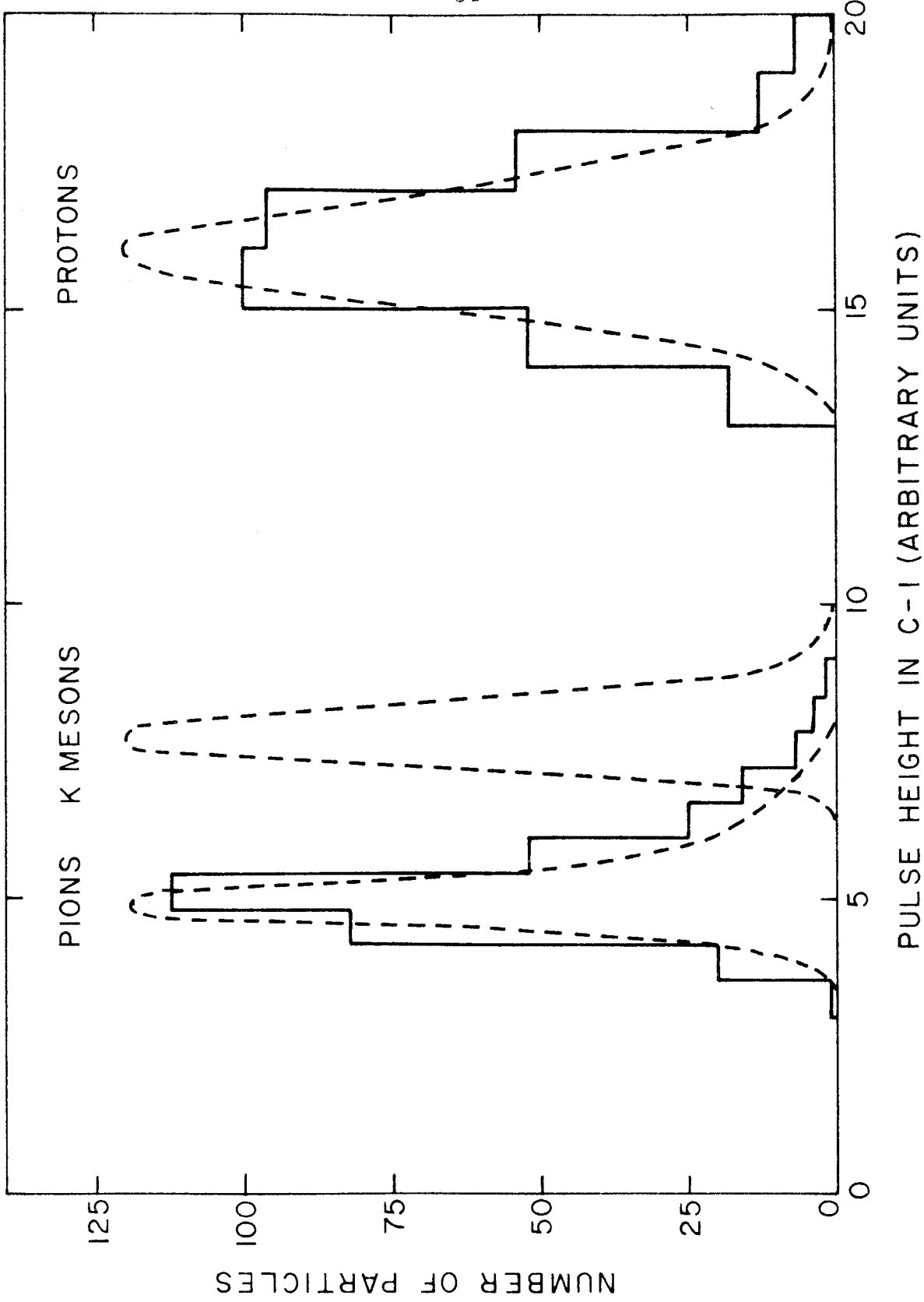
PROTONS
K MESONS
PIONS
NUMBER OF PARTICLES
0
25
50
75
100
125
0
5
10
15
20
PULSE HEIGHT IN C-1 (ARBITRARY UNITS)

allows the separation of the peaks quite easily.

The Liquid Hydrogen Target

This target was designed largely by V. Z. Peterson, who was assisted in its development and maintenance by E. B. Emery. A portion of this target is shown in figure 3. The liquid hydrogen, whose density was 0.0726 during this experiment, is contained in a thin-walled Mylar cup 3 inches in diameter. Surrounding this cup are several thin aluminum and copper heat shields in thermal contact with a liquid hydrogen reservoir. A Mylar window 0.024 inch thick surrounds the whole system.

In passing through the target the bremsstrahlung must traverse a total thickness of Mylar equivalent in the total number of protons to 15.7 per cent of the total liquid hydrogen traversed. Most of the particles produced in this Mylar cannot be counted, however, because they cannot pass through both C-0 and the magnet aperture. At 15 degrees this is not true, and a background correction for the Mylar must be made.

Because of the width of the bremsstrahlung beam, about 2 inches, not all photons pass through the full 3 inch diameter of the target. The actual density of photons as a function of their position in the target was measured photographically during this experiment. The effective length of the target was calculated from these measurements to be 2.78 inches.

Electronics

The electronic requirements of this experiment are typical of those encountered in most experiments making use of a pulsed particle accelerator such as the electron synchrotron at the California Institute of Technology. The bremsstrahlung beam from this machine occurs in bursts of about 20 milliseconds duration approximately once per second. This necessitates counting equipment capable of efficient, reliable operation at fairly high counting rates for relatively short periods of time. The low duty cycle, however, makes it possible to reduce greatly the time-independent sources of background by gating the counting equipment "off" during the beam-off time.

The electronic system used in this experiment is shown in block form in figure 7. Many of its components are of conventional design and are standard Synchrotron Laboratory equipment. These include: pulse amplifiers, Model 522A, with rise time of about 0.07 microsecond and maximum gain of 2500; coincidence circuit, Model 100, with three discriminator-equipped inputs and a resolving time of about 0.1 microsecond; photomultiplier preamplifier, Model 24, with square output pulses proportional in voltage amplitude to the input charge and 0.3 microsecond in length; scalers, Model 2, decimal units for counting rates less than 10 kcs. A discussion of the system as a whole precedes a detailed description of its performance.

Signals from C-0 and C-2 are transported through coaxial cables (Type RG 63/U, characteristic impedance 125 ohms) to the inputs of the fast coincidence circuit without amplification. A variable

Figure 7. Electronics Block Diagram.

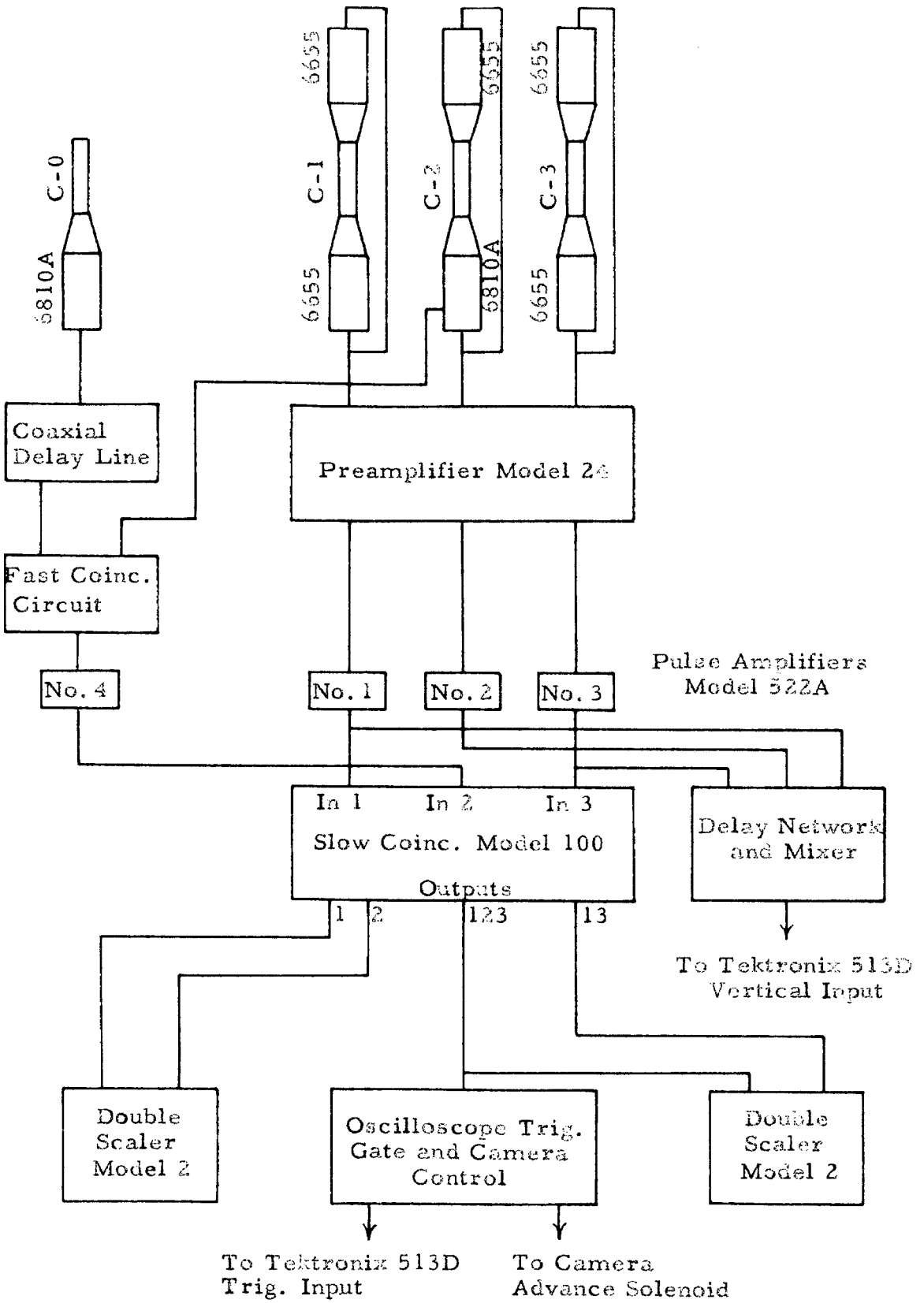
C-0
6810A
C-1
6655
6655
C-2
6655
6810A
C-3
6655
6655
Coaxial Delay Line
Preamplifier Model 24
Fast Coinc. Circuit
No. 4
No. 1
No. 2
No. 3
Pulse Amplifiers Model 522A
In 1
In 2
In 3
Slow Coinc. Model 100
Outputs
1
2
123
13
Delay Network and Mixer
To Tektronix 513D Vertical Input
Double Scaler Model 2
Oscilloscope Trig. Gate and Camera Control
Double Scaler Model 2
To Tektronix 513D Trig. Input
To Camera Advance Solenoid

coaxial delay line is inserted between C-0 and the fast coincidence circuit and is adjusted to the correct length for K mesons of the correct momentum, as explained in section II. The output of the fast coincidence circuit, henceforth called F, is amplified and brought to one input of the Model 100 "slow" coincidence circuit. Signals from C-1 and C-3 are amplified and brought to the remaining inputs. A 1-F-3 coincidence at this circuit is used to trigger the sweep of a Tektronix 513D oscilloscope whose trace then displays the pulses from C-1, C-2, and C-3, which are delayed relative to one another and mixed. Thus, a K^+ meson passing through all counters with the correct velocity causes the display of pulses proportional to its energy loss in the three counters. These pulses are photographically recorded for future analysis as explained in section V.

There are two major requirements which the fast coincidence circuit must satisfy: it must be capable of resolving pulses separated by more than 4 millimicroseconds; it must also be capable of reliable operation at a singles counting rate in one channel of approximately 5×10^6 counts per second during each beam pulse. In order to obtain the desired resolving time it is necessary to have input signals whose leading edge is defined to within one or two millimicroseconds. Consequently, RCA Type 6810A photomultipliers, capable of delivering current pulses of 40 to 50 milliamperes amplitude, were used on C-0 and C-2. A 5-volt pulse capable of operating the fast coincidence circuit was thus obtained in the 125 ohm coaxial cable used. The rise time of these pulses was largely determined by the transit time spread

in the photomultipliers, the light collection system, and the inductance of the photomultiplier output circuit. Although the rise time could not be measured directly, it was estimated to be 3 or 4 millimicroseconds. Since the fast coincidence circuit, as explained below, requires only a 0.5 volt pulse for operation, these pulses satisfy the requirement of being defined to 1 or 2 millimicroseconds for the purpose of the coincidence measurement. In order to avoid lengthening the rise time unnecessarily, all cables carrying the fast-rising pulses were soldered directly into the circuits with which they were associated, thus avoiding distributed capacitance in the form of standard coaxial fittings.

A schematic diagram of the fast coincidence circuit is shown in figure 8. This circuit is based on one in use at the University of California Radiation Laboratory at Berkeley. A negative signal on input 1 only is sufficient to turn V-1 off completely. When the 20-milliampere plate current is turned off, the voltage at the plate rises at a rate i_p/c_p, where c_p is the distributed plate capacitance, about 10 picofarads. Because of the effective 63 ohm plate load resistance, due to the parallel combination of the clipping stub and its termination, a 1.25 volt pulse rising in less than 1 millimicrosecond is obtained. This pulse is clipped to a length of 2.5 millimicroseconds. Diodes D-1 and D-2 normally conduct 1 milliampere each. The positive pulse applied to the cathode of D-1 turns it off, forcing its current through D-2 and causing thereby a rise in the potential at point A of 0.1 volt. Coincident signals at both inputs, however, shut off both diodes, causing the potential at A to rise linearly in time, reaching a value of 0.5 volt if

Figure 8. Fast Coincidence Circuit.

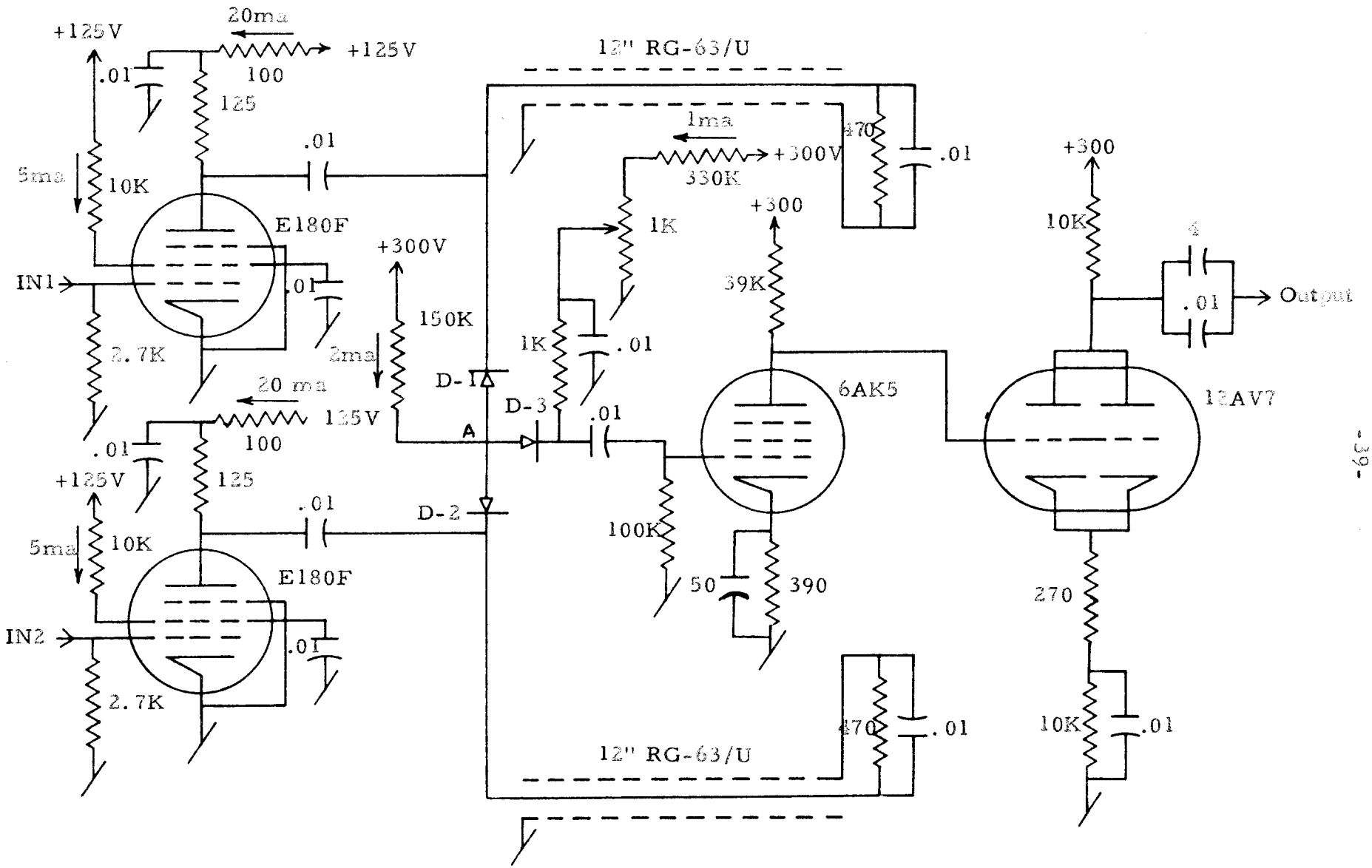
+125V
20ma
+125V
100
.01
125
12" RG-63/U
1ma
470
.01
+300V
330K
+300
5ma
10K
E180F
1K
+300
10K
4
IN1
.01
+300V
39K
.01
Output
150K
1K
.01
2.7K
2ma
D-1
6AK5
12AV7
20 ma
125V
D-3
.01
100
A
.01
+125V
125
.01
D-2
100K
5ma
10K
50
390
E180F
270
IN2
.01
2.7K
470
.01
12" RG-63/U
10K
.01

the input signals are exactly in coincidence. This coincidence signal, of course, decreases with increasing separation of the input pulses until the singles level is reached. The diode D-3 is normally biased "off" by about 0.1 volt to prevent singles pulses from feeding through to the following stretcher and output stages. The result is a triangular response function with a base width of 5 millimicroseconds and no singles feedthrough, even at the counting rate involved.

The actual performance of the fast circuit was measured by counting pions and protons with a suitable delay and comparing the counting rates obtained with this system to those obtained by requiring only a slow 1-2-3 coincidence. The latter were taken to be the "true" counting rates for both pions and protons, making possible a direct determination of the efficiency of the fast coincidence circuit. The relative response of the overall system using the fast circuit was then measured as a function of the delay between input signals. The response function of figure 9 was obtained. The response of the fast circuit was not as good as desired for the following reason: the times of arrival at the photomultiplier on C-2 of signals from particles of a particular type are distributed over an interval of 4 or 5 millimicroseconds because of their momentum spread, their various path lengths through the spectrometer, and the spread in light collection time in the large counters used. Since the total time spread is of the same order as the resolving time of the fast coincidence circuit, some particles are inevitably lost. The result is the triangular response function shown in figure 9. Taking the peak relative yields to be the

Figure 9. Response of Fast Coincidence Circuit.

This figure gives the response to pions and protons at a momentum of 468 Mev/c as a function of the relative delay between the signals from C-0 and C-2.

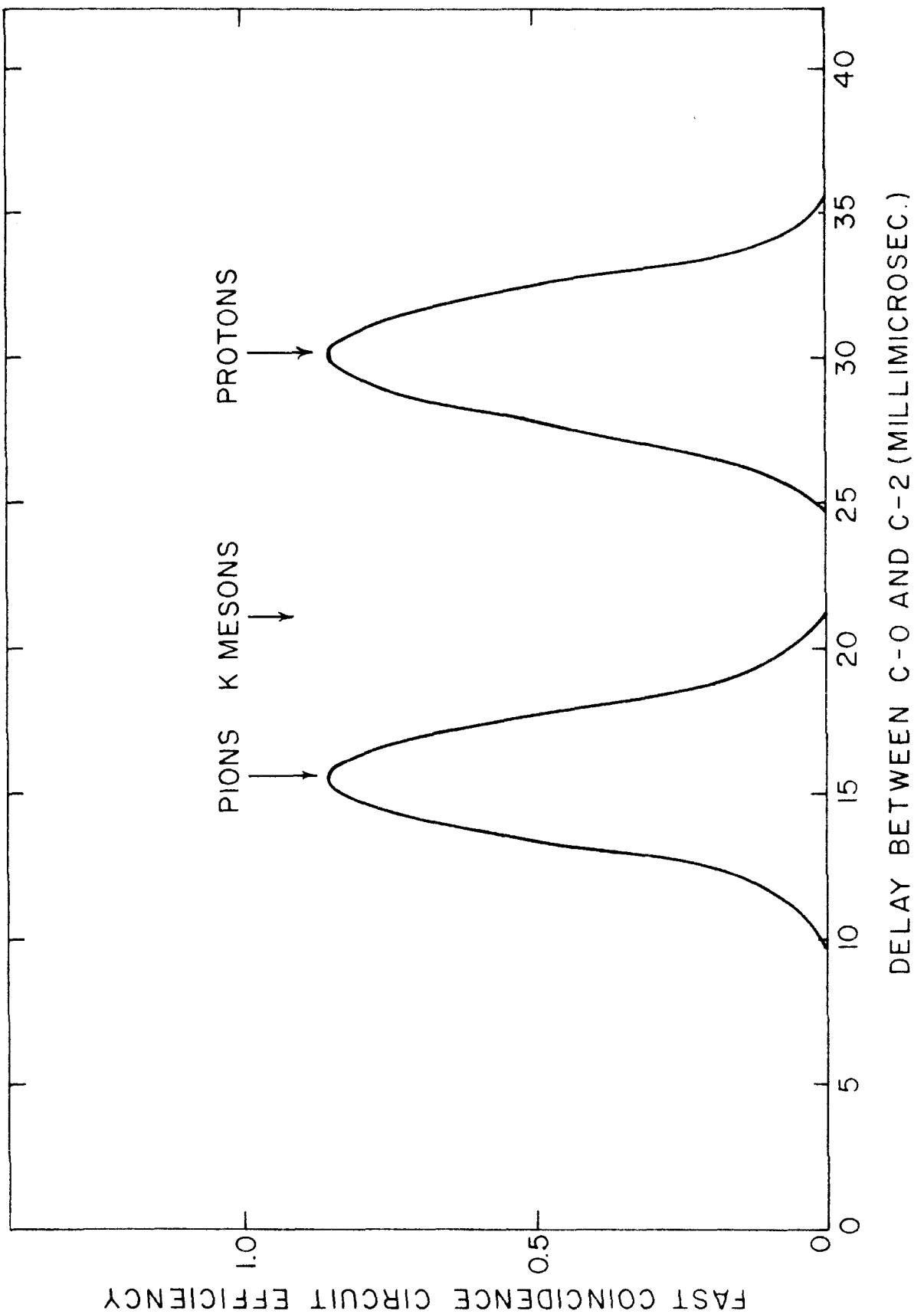
FAST COINCIDENCE CIRCUIT EFFICIENCY
1.0
0.5
0
0
5
10
15
20
25
30
35
40
DELAY BETWEEN C-0 AND C-2 (MILLIMICROSEC.)
PIONS
K MESONS
PROTONS

efficiency of the fast coincidence circuit, a value of 0.85 ± 0.01 for both protons and pions is obtained. This value is, by interpolation, used also for K mesons. For the earlier measurements the efficiency was not measured so accurately. Although changes in the photomultipliers during the course of the experiment may have had some effect on the efficiency, this effect is probably small, as judged from the measurements available from the early part of the experiment. Un fortunately, most of the K^+ mesons were counted at a delay which permitted from 1 to 2 per cent of the pions to be counted also, resulting in 10 to 20 pions counted for each K^+ meson.

Photographic Equipment

Pulses were recorded on Kodak Tri-X film, using a f:1.5 lens. The film was advanced automatically after each exposure. After development, the pulses were projected onto a screen from which accurate pulse-height measurements were made.

IV. EXPERIMENTAL PROCEDURE

Synchrotron Operation

Electrons are accelerated in the synchrotron at a repetition rate of one cycle per second. Bremsstrahlung having a well-defined endpoint energy is obtained by holding the magnetic field of the synchrotron constant during a 20-millisecond interval while the RF accelerating field is reduced in a controlled manner such that the electrons spiral into the tantalum radiator at a uniform rate. A bremsstrahlung beam of constant endpoint energy is thereby obtained. The bremsstrahlung is emitted over the full 20-millisecond interval in order to keep the accidental counting rate in counter experiments as low as possible. The "plateau" in the magnetic field may be set to any desired value, making it possible to obtain bremsstrahlung having any endpoint energy up to the present maximum of 1100 Mev, which is determined by RF voltage limitations. At 1100 Mev about 5 to 10 per cent of the electrons strike the radiator before the plateau is reached, resulting in a slight smearing of the endpoint energy. This necessitates a small correction to the data taken at a photon energy of 1060 Mev, as explained in section VI.

The energy of the electrons when they strike the radiator, which is equal to the bremsstrahlung endpoint energy, is monitored by a system due to M. Sands which measures the magnetic field of the synchrotron during the plateau. A knowledge of the field and the position of the radiator is sufficient to determine the electron energy. The accuracy of this system has been checked by Walker, Donoho, and

Emery (17), who used a pair spectrometer to measure the endpoint energy of the bremsstrahlung. This measurement agreed with the field monitor to a precision of 0.5 per cent. The total bremsstrahlung energy is measured by a Cornell-type thick-walled ionization chamber which has been calibrated by Gomez (18) against the energy-independent Quantameter of Wilson (19). The output current of the ionization chamber is integrated; a standard integrator unit is the BIP (Beam Integrator Pulse), which is equivalent to a total bremsstrahlung energy of 1.15×10^{12} Mev.

The energy spectrum of the bremsstrahlung has also been measured by Walker, Donoho, and Emery with the pair spectrometer (17). Although a fairly thick radiator (0.2 radiation length) is used in the synchrotron, the measurements, though not yet completely analyzed, indicate a spectrum very close to the theoretical "thin-target" spectrum. Since a calculated spectrum for the thickness of the radiator used, calculated by D. Elliott (20), differs considerably from the measured spectrum, it is thought that the electrons spiral very slowly into the radiator so that the bremsstrahlung is all produced in the rounded edge of the radiator, where the electrons "see" an effectively thin radiator. The measurements determine essentially the quantity $B(E_o, k/E_o)$ which is defined by the expression

$$n(k)dk = \frac{W}{E_o} B(E_o, k/E_o) \frac{dk}{k} , \qquad (6)$$

where $n(k)dk$ is the number of photons in the interval k to $k + dk$ for a bremsstrahlung beam of total energy W and endpoint energy E_o. The

pair spectrometer measurements indicate no variation in the quantity $B(E_o, k/E_o)$ over the range $k/E_o = 0.6$ to $k/E_o = 1.0$. For the purpose of the calculations necessary to this experiment, the value 0.90 has been adopted for $B(E_o, k/E_o)$. A small correction in this quantity will, perhaps, be needed when the pair spectrometer data are completely analyzed.

Experimental Layout

A schematic plan view of the experimental area is shown in figure 10. The bremsstrahlung is collimated in one leg of the synchrotron magnet yoke by the lead primary collimator. For the first part of this experiment this collimator had a circular aperture which did not limit the beam enough to prevent its hitting the metal fittings on the hydrogen target. Consequently, a secondary collimator, at A, further reduced the beam such that it was confined to the central portion of the target. At the end of the experiment the primary collimator had been replaced by one which had a rectangular aperture such that the secondary collimator served only to scrape the edges of the beam without actually doing any collimation. Immediately following the primary collimator was an 8-inch-thick lead wall which stopped much of the stray radiation produced in the walls of the primary collimator. The beam passed through a gaseous hydrogen target which was used in other experiments. Following this target was the secondary collimator, which was followed by a magnetic field to sweep charged particles out of the line of the beam. A final scraper placed 1 meter in front of the liquid hydrogen

Figure 10. Plan View of the Experimental Area.

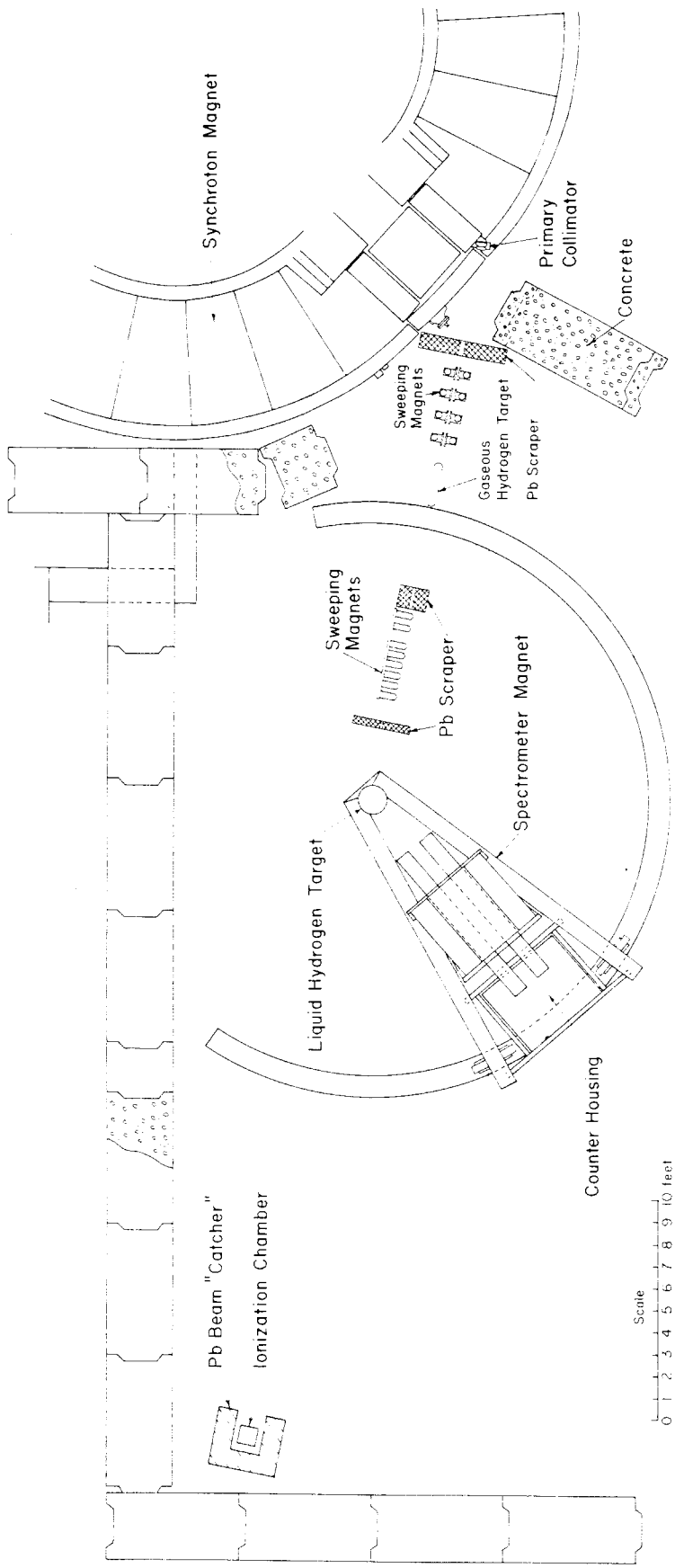
Synchroton Magnet
Primary Collimator
Concrete
Sweeping Magnets
Gaseous Hydrogen Target
Pb Scraper
Sweeping Magnets
Pb Scraper
Spectrometer Magnet
Liquid Hydrogen Target
Counter Housing
Pb Beam "Catcher"
Ionization Chamber
Scale
0 1 2 3 4 5 6 7 8 9 10 feet

target prevented radiation from striking the metal fittings of the target. After passing through the target, which is located 33 feet from the radiator, the beam struck the monitor, which is 56 feet from the radiator.

At the target the beam is rectangular in cross section, approximately 2 inches wide and 2 1/2 inches high, thus insuring that only the central portion of the target is irradiated. Because of the cylindrical shape of the target, as explained in section III, the average target length traversed by the bremsstrahlung is only 2.78 inches.

Experimental Operation

The choice of K^+ meson laboratory angle and momentum was governed by several factors. Since the observed K^+ mesons were expected to come from the reaction

$$\gamma + P \rightarrow K^+ + \Lambda^o \qquad (1)$$

it seemed most logical to select values for the photon energy and K^+ meson C.M. angle for this reaction and to make observations at the corresponding K^+ meson laboratory angle and momentum. In this way an angular distribution at constant photon energy or an energy excitation function at constant C.M. angle can be measured. This method of selection was generally followed, but restrictions upon the ranges of angles and energies at which measurements could be made were imposed by the 1100 Mev bremsstrahlung endpoint and by limitations in the detection equipment.

An upper limit to the momentum at which measurements could be made was imposed by the 600 Mev/c limit of the spectrometer. Actually, the highest momentum at which measurements were made was 520 Mev/c; the time-of-flight discrimination and pulse-height resolution deteriorated rapidly above this momentum. An absolute lower limit to the momentum came from the requirement that K^+ mesons be counted in all the counters. For the total thickness of the counters used K^+ mesons of momentum greater than 250 Mev/c were required. Thinner counters could, of course, be used, but a practical lower limit to the momentum of 320 Mev/c was imposed by the counting rate sensitivity of the spectrometer. The K^+ meson counting rate, because of dynamical factors, falls with decreasing momentum approximately as the cube of the momentum. In addition, the decay in flight of the K^+ mesons becomes very large at low momenta, reaching 85 per cent at a momentum of 320 Mev/c.

The angular limitations to the range of measurements were not serious. The front counter required operation at 15 degrees or greater in order to keep the counting rate low. Although the beam struck the magnet frame at 15 degrees, thereby increasing the stray background greatly, reliable operation was obtained by placing a three inch carbon absorber between the counter and the target and shielding the counter from the beam-line with a four inch thickness of lead.

Figure 11 shows the kinematics of the reaction of interest, reaction 1. Plotted there are curves relating laboratory angle and momentum both for constant photon energy and for constant C. M. angle.

Figure 11. Kinematics of the Reaction $\gamma + P \rightarrow K^+ + \Lambda^o$

This figure shows K^+ meson laboratory momentum as a function of laboratory angle for constant photon energy and constant C. M. angle. The sensitive region of the spectrometer is shown for each point at which measurements were made.

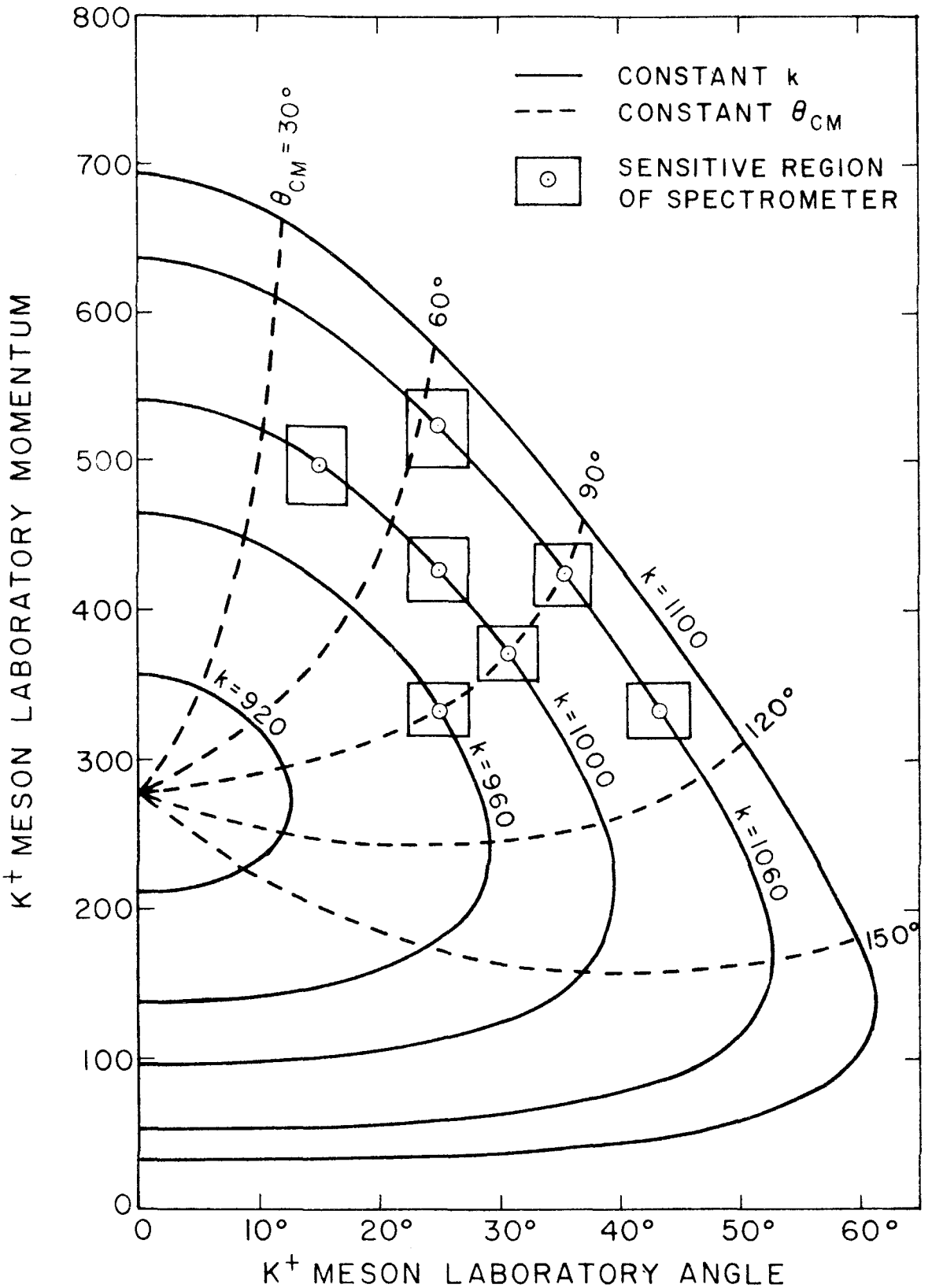
CONSTANT k
CONSTANT θ_{CM}
SENSITIVE REGION OF SPECTROMETER
θ_{CM} = 30°
60°
90°
120°
150°
k=920
k=960
k=1000
k=1060
k=1100
800
700
600
500
400
300
200
100
0
0
10°
20°
30°
40°
50°
60°
K+ MESON LABORATORY MOMENTUM
K+ MESON LABORATORY ANGLE

The points where measurements were made are indicated, together with the sensitive region of the spectrometer for each point. These points are consistent with the plan stated above: three C.M. angles at each of 1060 Mev and 1000 Mev were observed and three energies at 90 degrees C.M. were observed.

In order to eliminate protons of the same momentum as the K^+ mesons being counted, protons were always stopped before reaching C-3. At momenta up to 375 Mev/c counters C-1 and C-2 were alone sufficient to stop the protons, but at higher momenta additional absorbers between C-1 and C-2 and between C-2 and C-3 were needed. Lead and carbon absorbers were used for this purpose, up to 0.75 inch of lead being required. The between-counters absorbers served other useful purposes: they also stopped low-energy particles not coming through the magnet, thereby reducing the accidental rate somewhat; and they slowed K^+ mesons relative to pions, providing better pulse-height resolution for the K^+ mesons. A major disadvantage to the use of these absorbers was the fact that pion interactions in the absorbers might give rise to events which could be interpreted in the following counters as K mesons. For this reason no absorber was ever placed in front of C-1, insuring a "normal" pulse-height spectrum in this counter. Because of multiple Coulomb scattering in the absorbers a small correction to the counting rate was made necessary when the absorber was placed between C-1 and C-2. This correction, which is due mainly to the scattering of K^+ mesons out of C-3 never exceeded about three per cent. The correction is discussed also in section VI,

as is the correction due to nuclear absorption both in the absorbers and in the counters.

Data were taken in "runs" consisting of several hundreds of BIP's (see Synchrotron Operation, this section). When possible, background runs were interspersed between the K^+ meson runs in order to insure that they were taken under the same conditions. Because of the difficulty of scheduling the operating energy to suit all experiments, this was not always possible. The ease of setting the spectrometer to a desired point, however, made this no serious defect in the experiment.

During each run the bremsstrahlung endpoint was monitored frequently, as was the field of the magnetic spectrometer. There was never appreciable drift in these quantities during the course of a run.

V. IDENTIFICATION OF K^+ MESONS

The raw data obtained from each experimental run consisted of several hundreds of photographically recorded oscilloscope traces each due to a particle which satisfied the requirements of the detection system, as explained in the preceding sections. From 80 to 95 per cent of these traces were due to pions, the remainder being almost equally divided between K^+ mesons and particles whose identity is not known but which are probably the scattered protons discussed in section II. This section is concerned with the determination, by means of pulse-height analysis of the raw data, of the counting rate for K^+ mesons at each experimental point. The general method of analysis consists in setting limits for each counter between which the pulse height for a K^+ meson must lie. By the requirement that the pulse in each counter lie in the proper interval for a particle to be identified as a K^+ meson, good discrimination against background particles is obtained.

As soon as the photographic processing of each run was completed, the oscilloscope traces were projected onto a screen from which the pulse heights in each counter were recorded, preserving the correlation among the three counters for each particle, of course. The three single-counter pulse-height spectra were then plotted, more to obtain from the pion spectrum a calibration of the pulse height distributions for minimum-ionizing particles than to resolve by this means the K^+ mesons. Because of the predominance of pions an accurate determination of their most probable pulse height was obtained, permitting a calculation of the most probable pulse height for K^+ mesons

in each counter.

Actually, more information about the K^+ meson pulse-height distributions was known than the mere position of the most probable pulse height. From measurements on the distributions of pions and protons at a momentum of 468 Mev/c the standard deviations of the pulse-height distributions for these particles were obtained, the following values being observed:

$$\sigma_\pi(1) = 0.15\,\mu_\pi(1) \qquad \sigma_p(1) = 0.06\,\mu_p(1)$$

$$\sigma_\pi(2) = 0.15\,\mu_\pi(2) \qquad \sigma_p(2) = 0.06\,\mu_p(2)$$

$$\sigma_\pi(3) = 0.21\,\mu_\pi(3) \qquad \sigma_p(3) = 0.08\,\mu_p(3)$$

In these relationships $\sigma(n)$ is the standard deviation in counter n, and $\mu(n)$ is the most probable pulse height in the same counter. From these values an estimate of the spread in the K^+ meson distribution in each counter was made for each run. Although there were never enough K^+ mesons in a single run to provide an accurate check of these estimates, rough agreement was always obtained, establishing a degree of confidence in the number of K^+ mesons obtained.

Counters C-1 and C-2, having the best resolution, were used as the primary means for identifying K^+ mesons, C-3 used as only a not-too-restrictive check against the results obtained with C-1 and C-2. A very simple means of emphasizing the separation between the K^+ mesons and the background in these counters was employed. Each particle in a run was represented as a point on a chart, its position

being determined by the pulse heights in C-1 and C-2. Logarithmic scales were used for the coordinate axes, emphasizing the fact that the relative dispersion of the K^+ mesons is smaller than that of the pions, even though their absolute dispersion may be greater. The logarithmic scales, therefore, have the effect of presenting the K^+ mesons as a tighter group than the pions and, at the same time, displaying the separation between the two groups effectively. Other background, namely the "scattered protons", do not form a definite grouping, although the density of these particles is greater at pulse heights larger than those of the K^+ mesons.

For all experimental runs it was possible in this way to identify a definite group of K^+ mesons. The distributions of the pulses in these two counters always fell within the predicted range. For each pulse in the groups identified as K^+ mesons the pulse height in C-3 was examined. If it deviated by more than two standard deviations from the expected mean, the particle was rejected. In general the rejected particles were on the border of the group in the other two counters also. The number of K^+ mesons rejected in this way should be quite small. It is estimated that no more than 5 per cent are rejected on the basis of the method of selection.

Typical log-log charts for runs taken at momenta of 320 Mev/c, 425 Mev/c, and 520 Mev/c are shown together with their corresponding background runs in figures 12, 13, and 14 respectively. These examples illustrate the problems encountered in the interpretation of the data over the whole range of momenta. At 420 Mev/c, figure 13, the

Figure 12. Pulse-Height Correlation Between C-1 and C-2.

p_o = 320 Mev/c, θ_{lab} = 25°, k = 960 Mev

E_o = 920 Mev, 3000 BIP's (background)

E_o = 1080 Mev, 6000 BIP's

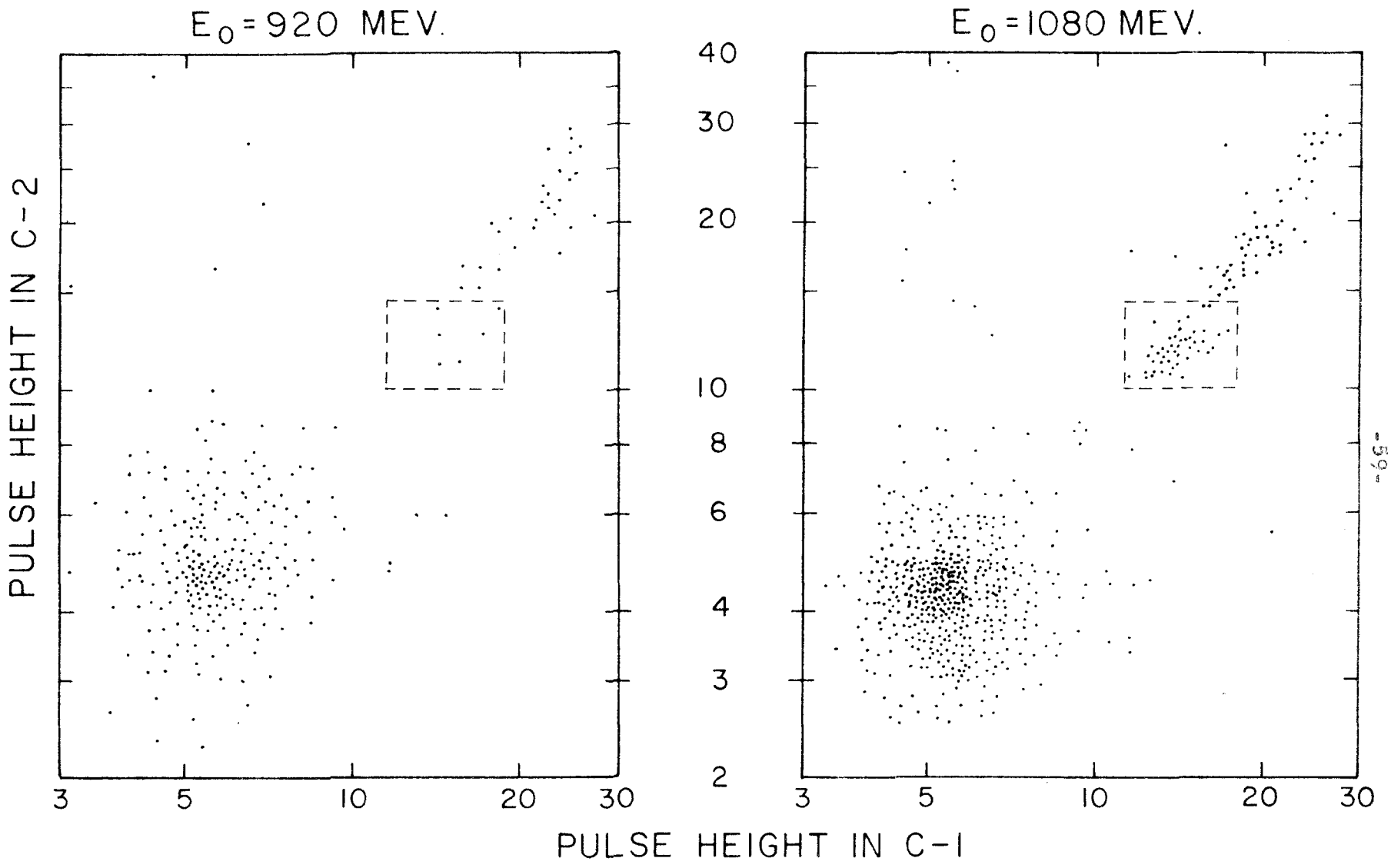
E_0 = 920 MEV.
E_0 = 1080 MEV.
PULSE HEIGHT IN C-2
PULSE HEIGHT IN C-1
40
30
20
10
8
6
4
3
2
3
5
10
20
30

Figure 13. Pulse-Height Correlation Between C-1 and C-2.

p_o = 425 Mev/c, θ_{lab} = 15°, k = 1000 Mev.

E_o = 940 Mev, 2400 BIP's, (background)

E_o = 1100 Mev, 5000 BIP's

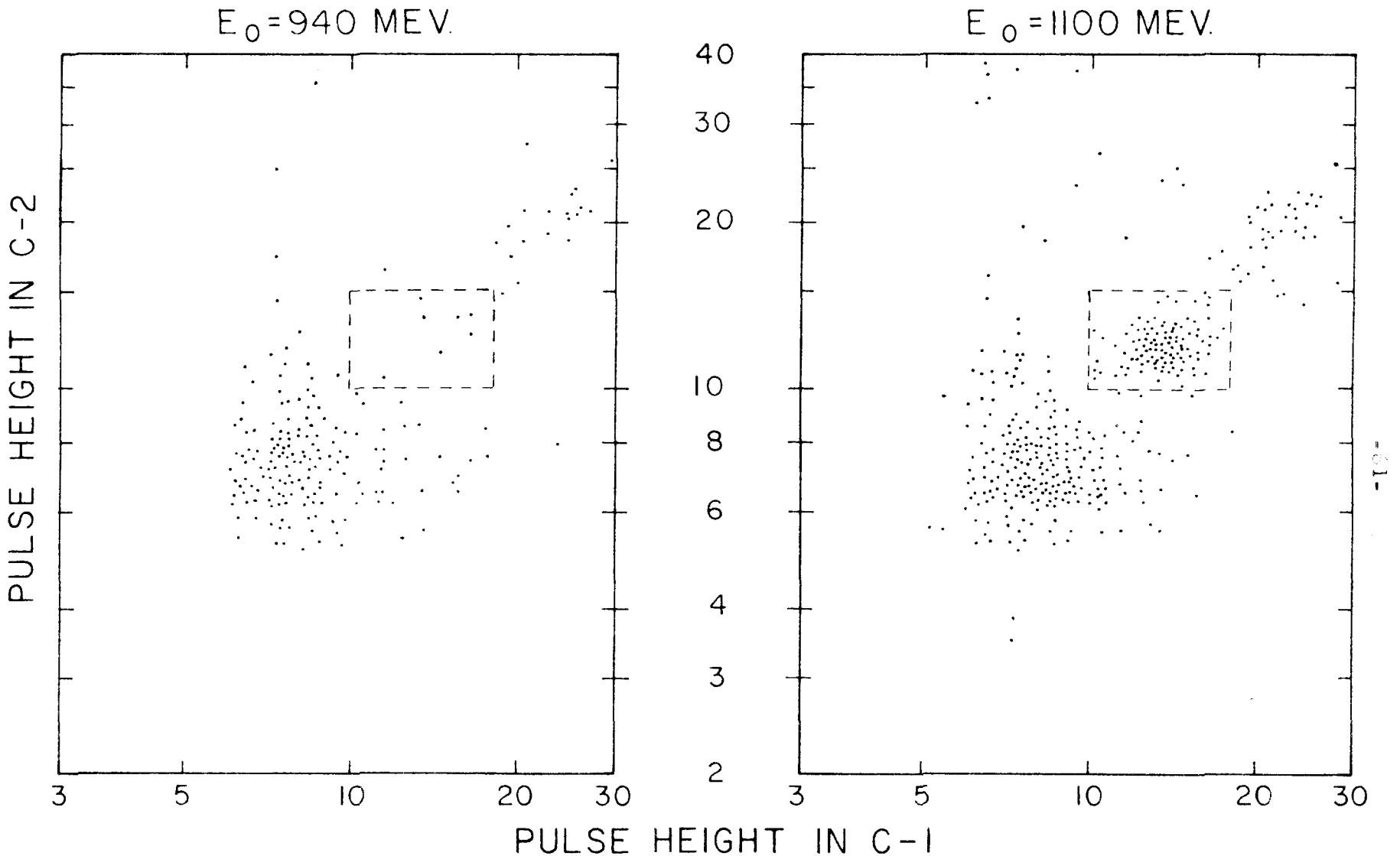
E 0 = 940 MEV.
E 0 = 1100 MEV.
PULSE HEIGHT IN C-2
PULSE HEIGHT IN C-1
40
30
20
10
8
6
4
3
2
3
5
10
20
30

Figure 14. Pulse-Height Correlation Between C-1 and C-2.

p_o = 520 Mev/c, θ_{lab} = 25°, k = 1060 Mev

E_o = 1000 Mev, 1200 BIP's, (background)

E_o = 1100 Mev, 2400 BIP's

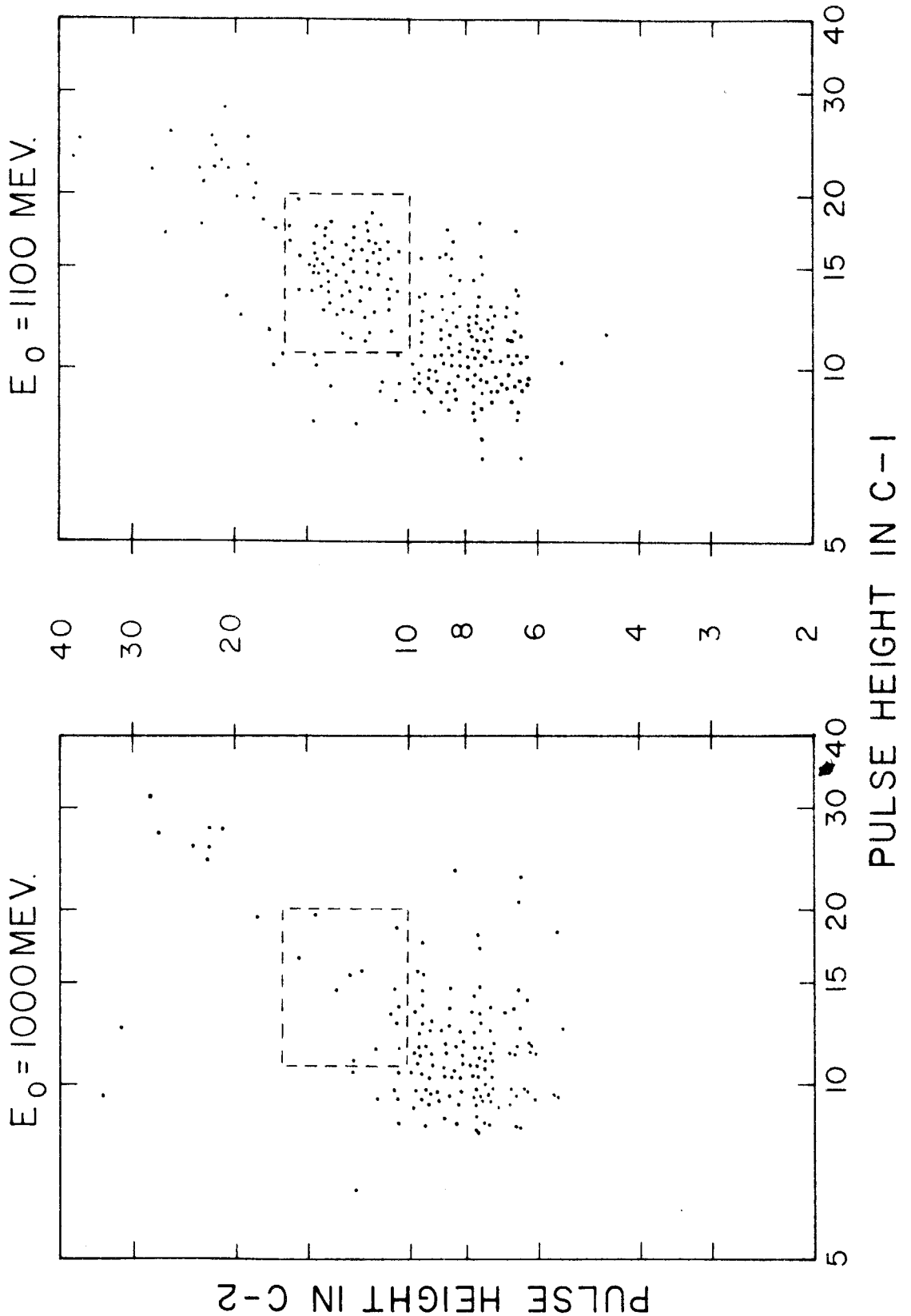
E_0 = 1100 MEV.
E_0 = 1000 MEV.
PULSE HEIGHT IN C-1
PULSE HEIGHT IN C-2
5
10
15
20
30
40
2
3
4
6
8
10
20
30
40

situation is almost ideal. There is very good separation between the K^+ mesons and the pions with very little interference from the "scattered protons", which are also clearly separated from the K^+ mesons. Indeed, no particles in the K^+ meson group were rejected on the basis of the evidence from C-3. The background for this run amounted to only 10 per cent of the K^+ meson yield. At 320 Mev/c, figure 12, the separation between K^+ mesons and pions is improved, but the K^+ meson group is subjected to some interference from the "scattered protons". About 5 per cent of the particles in the group were rejected on the basis of C-3. The background was, nevertheless, about 25 per cent, as high as at any point measured. The 520 Mev/c point, figure 14, exhibits the opposite difficulty; the separation between pions and K^+ mesons is not very clear. About 10 per cent of the particles were rejected on the basis of C-3, but the background was, nevertheless, 25 per cent. An important feature of these charts is that the yields of pions and protons in the background runs are roughly the same as in the K^+ meson runs, giving justification to the assumption that these sources of background do not change when the synchrotron energy is lowered.

The counting rate for K^+ mesons for each experimental point together with the background counting rate is listed in Table II. The counting rates are expressed as the number of particles per hundred BIP's. The errors shown are standard deviations based only on counting statistics.

Table II. K^+ Meson Counting Rates

P_o Mev/c	θ_{LAB} Degrees	k Mev	$\theta_{C.M.}$ Degrees	E_o Mev	Counting Rate K Mesons/100 BIP's*
335	25.1	960	90	1080	0.51 ± 0.09
				920	0.14 ∓ 0.05
372	30.6	1000	90	1100	0.69 ± 0.08
				940	0.12 ∓ 0.06
427	25.0	1000	72	1100	1.30 ± 0.19
				940	0.06 ∓ 0.06
499	15.0	1000	42	1100	1.79 ± 0.18
				940	0.21 ∓ 0.09
336	43.3	1060	110	1100	0.24 ± 0.06
				1000	0
422	35.6	1060	90	1100	0.95 ± 0.13
				1000	0.09 ∓ 0.09
523	25.0	1060	64	1100	2.98 ± 0.31
				1000	0.52 ∓ 0.20

* 100 BIP's = 1.15×10^{14} Mev integrated bremsstrahlung energy.

VI. CALCULATION OF CROSS SECTIONS

This section is concerned with the conversion of the counting rates derived in the preceding section into differential C.M. cross sections for $K^+ - {}^{o}$ photoproduction. The basic relationship between counting rate and cross section is first presented. Corrections to this basic relationship due to scattering, absorption, decay in flight, detection efficiency, and premature beam dump are then described. The cross sections are calculated, finally, and the sources of error in this experiment are discussed.

Counting Rate-Cross Section Relationship

Since the initial and final states of the reaction of interest, namely

$$\gamma + P \rightarrow K^+ + \Lambda^{o} \tag{1}$$

contain exactly two particles each, a knowledge of the momentum and direction of the K^+ meson is sufficient to determine completely the kinematics of the reaction. The photon energy, k, the K^+ meson momentum, p, and the K^+ meson angle, θ, are related by the following equation:

$$k = \frac{M_P E + (M_\Lambda^2 - M_P^2 - M_K^2)/2}{M_P + p\cos\theta - E} \tag{7}$$

M_P is the proton mass, M_K is the K meson mass, M_Λ is the Λ^{o} hyperon mass, and E is the K meson total energy. The C.M. angle, θ', is related to the laboratory coordinates by the expression:

$$\tan \theta' = \frac{\sin \theta \sqrt{1 - \beta_o^2}}{\cos \theta - \beta_o/\beta} \tag{8}$$

In this expression, β_o is the velocity of the C.M. system with respect to the laboratory system, and β is the K^+ meson laboratory velocity. The Jacobian for the transformation from the C.M. system to the laboratory system, $\partial \Omega' / \partial \Omega$, is obtained by differentiating the above expression.

The differential C.M. cross section for the reaction may be expressed as $\sigma(\theta', k)$, a function of both θ' and k (or θ and p). For the case where the cross section is not a rapidly varying function of angle or energy, as seems to be the case for this reaction, the following expression relating the counting rate to the cross section is valid:

$$C = \sigma \frac{\partial \Omega'}{\partial \Omega} \Delta\Omega \, \rho \bar{\ell} \, n(k) \Delta k \, RA \tag{9}$$

The terms of this expression are explained below:

C: the number of particles counted per 100 BIP's.

$\sigma (\partial \Omega'/\partial \Omega) \Delta\Omega$; the cross section for emitting K^+ mesons into the solid angle of acceptance of the spectrometer per proton per incident photon of energy k.

$\rho \bar{\ell}$: the number of protons per cm^2 interacting with the bremsstrahlung beam. ρ is the number of protons per cm^3 and $\bar{\ell}$ is the effective target length.

n(k): the number of photons of energy k per unit photon energy interval per 100 BIP's, as given by equation 6, section IV.

Δk: the photon energy interval which contributes K^+ mesons within the momentum acceptance interval of the spectrometer. This can be written in terms of the spectrometer momentum interval as $\Delta k = \frac{\partial k}{\partial p} P_o \frac{\Delta p}{p_o}$, where $\frac{\partial k}{\partial p}$ is obtained by differentiation of equation 7.

R: a correction factor due to the decay in flight of K mesons.

A: a correction factor due to all other effects.

It should be mentioned that this expression is only approximate, since it treats all functions of p and θ as constant over the range of acceptance of the spectrometer. If it is desired to take this variation into account, equation 9 may be rederived in a more exact fashion. In this case the expression relating counting rate and cross section becomes a rather complicated integral which must be solved by numerical means. This integral has been derived for the spectrometer used in this experiment, and a program for its computation using the Datatron digital computer has been prepared (15). Although such exactness is not necessary in general for this experiment, because of the large probable errors in the determination of the counting rates, this program takes into account such factors as the effect of energy loss in the front absorber and in the target on the momentum acceptance interval of the spectrometer and premature beam dump. It was, consequently, used to calculate the counting rate-cross section conversion factor for the 1060 Mev points and for the points where there was more than one-half inch of polyethylene placed before C-0. For these cases the more exact calculation differed by about 10 per cent from the simple expression given in equation 9.

The value calculated for the conversion factor for each experimental point is listed in Table 3, where it is referred to as $G(p, \theta)$.

Corrections

Detection System Efficiency. In section III it is stated that the efficiency of the fast coincidence circuit for detecting K^+ mesons is 0.85. The uncertainty in this number is only 0.01 for the most recent data, which includes the following points:

θ'	k
42^o	1000 Mev
90^o	960 Mev
110^o	1060 Mev

For all other points this uncertainty is not accurately known, but is estimated to be 0.05. This correction, 0.85, appears in the cross section determination in the term A, described above.

Decay in Flight. The most recent determination of the K^+ meson lifetime gives a value of 12.4 ± 0.2 millimicroseconds (5). A fraction of the K^+ mesons, therefore, decay in flight although they would otherwise be counted. The fraction surviving over the 165 inch distance between foci is given by the following expression:

$$R = e^{-556/p} \tag{10}$$

where p is the K^+ meson's momentum in Mev/c.

Nuclear Absorption. The K^+ mesons were required to traverse the 6 cm of polystyrene of which the counters were composed. In

addition, various absorbers of carbon and lead were placed at times in the path of the K^+ mesons. The total interaction cross sections in nuclear emulsions have been measured by several groups (9). The cross section per nucleon is 10 millibarns, about one-fourth of the geometrical cross section for a nucleon. The corrections needed are the following:

Absorber	Correction
Counters	2.7 °/o
1/2-inch lead	1.4 °/o
1-inch carbon	1.0 °/o

Scattering in Between-Counters Absorbers. The counters C-1, C-2, and C-3 were separated by about 6 inches. When absorbers were placed between these counters, they could cause scattering out of the counters which followed the absorbers due to multiple Coulomb scattering. This correction was, in general, quite small, being greater than one per cent only for the case when a half-inch lead absorber was placed between C-1 and C-2. The necessary correction was calculated through the use of formulas developed by R. L. Walker (21). A correction of 3.4 per cent was needed when this absorber was used and K^+ mesons of momentum 425 Mev/c were counted.

Scattering Before Entering Magnet. Multiple Coulomb scattering in C-0 and the absorber placed between C-0 and the target was not a source of appreciable correction. Since all scattering material was located as close as possible to the target and, consequently, subtended

a much larger solid angle than the magnet aperture, the scattering of particles out of the spectrometer is almost exactly balanced by scattering into the spectrometer of particles which otherwise would not have been counted. As a check of this assumption, the counting rate for pions was measured at a momentum of 310 Mev/c both with and without an absorber before C-0. Except for a small difference in counting rate attributable to nuclear absorption no difference was observed.

Premature Beam Dump. With the plateau of the synchrotron's magnetic field adjusted to a value corresponding to 1100 Mev, approximately 10 per cent of the electrons were dumped prematurely because of insufficient R.F. voltage. Since this premature dump took place within 25 Mev of the plateau, a correction was necessary only for the 1060 Mev points. By a consideration of the portion of the sensitive region of the spectrometer which extended into the region of premature dump, a correction of 3 per cent was calculated and applied to the 1060 Mev points only. Actually, this correction is automatically applied if the computer program described above is used.

The Cross Sections

The cross sections, as calculated from the counting rates of Table II, are listed in Table III. Also listed are the values calculated for the conversion factor $G(p, \theta)$. The corrections are listed, the decay-in-flight correction, R, being separated from the other corrections which are lumped together into the term A. The errors listed in this table are standard deviations based only on counting statistics. Other

Table III. Differential Cross Sections for the Reaction $\gamma + P \rightarrow K^+ + \Lambda^\circ$

k Mev	θ' Degrees	Net Counting Rate Counts/100 BIP's	$G(p, \theta)$ ster cm^{-2} / 100 BIP's	Corrections Decay	Corrections All Other	$\sigma(\theta', k)$ 10^{-31} cm^2/ster.
960	90	0.37 ± 0.11	1.86×10^{31}	0.169	0.82	1.38 ± 0.41
1000	42	1.35 ± 0.17	3.12×10^{31}	0.284	0.80	1.89 ± 0.24
1000	72	1.24 ± 0.19	2.68×10^{31}	0.259	0.80	2.18 ± 0.33
1000	90	0.57 ± 0.10	1.93×10^{31}	0.208	0.82	1.71 ± 0.27
1060	63	2.46 ± 0.37	3.52×10^{31}	0.336	0.78	2.57 ± 0.38
1060	90	0.86 ± 0.15	2.35×10^{31}	0.259	0.80	1.72 ± 0.30
1060	110	0.24 ± 0.06	1.13×10^{31}	0.169	0.80	1.52 ± 0.38

possible sources of error are discussed below.

Errors and Uncertainties

Counting statistics provide the largest source of error in this experiment. The relative probable errors from this source range between 15 and 35 per cent. In addition, the determination of the yields is subject to an unknown systematic error due to the method of taking background runs. It was assumed that the background due to protons and pions does not change if the synchrotron energy is lowered by a small amount. The fact that the yield of particles identified as background is roughly the same at both high and low synchrotron energies indicates that this assumption is correct, so that no error is assigned to the cross sections on this account.

The precision to which the other factors influencing the measurement of the cross section were known during the experiment greatly exceeds the precision to which the counting rates were known. The uncertainties in these quantities probably do not exceed 5 per cent.

VII. THEORY

Before any attempt at the interpretation of the results of this experiment it is useful to examine presently existing theory in order to determine how the most use may be made of the results.

There exist several points of similarity between $K^+ - \Lambda^o$ photoproduction and positive pion production in the reaction

$$\gamma + P \rightarrow \pi^+ + N \qquad (11)$$

The initial states of both reactions are identical and the final states both contain one meson and one baryon. If the K^+ meson is a pseudoscalar particle like the pion, then the similarity between the two processes is quite strong. Actually, experimental evidence, though far from conclusive, indicates that the K^+ meson does behave as a pseudoscalar particle in nuclear scattering. Analysis of the small-angle scattering of K^+ mesons in nuclear emulsions according to the optical model shows constructive interference between the nuclear scattering and the Coulomb scattering, indicating a repulsive nuclear potential (22). Stapp (23) has calculated the scattering of K^+ mesons by single nucleons using a Chew-type static, cut-off model. The result of this calculation indicates a repulsive nuclear potential for a pseudoscalar K^+ meson, but an attractive potential for a scalar K^+ meson. Although nuclear recoil should have a much larger effect in this case than in pion-nucleon scattering, the sign of the potential would reasonably be expected not to change when the effect of recoil is added. Consequently, it can be inferred from the scattering data, if somewhat weakly, that the K^+

meson is a pseudoscalar particle. Although no direct determination of the K^+ meson spin has yet been made, experimental evidence favors spin zero (24).

Since the pion photoproduction process is fairly well understood, a comparison of the results of this experiment to the cross section predicted by direct analogy to pion theory should be quite useful. There are, of course, differences between the two processes which may outweigh the similarities. For example, there is a strong attraction between the pion and nucleon in the state having $T = 3/2$, $J = 3/2$, yet the K^+ meson and the Λ^o hyperon can exist only in a state having $T = 1/2$. Interactions involving these particles would, therefore, not be expected to exhibit the strong 3/2 - 3/2 resonance observed in pion photoproduction and scattering. In addition, since the ratio of the K^+ meson mass to that of the nucleon is much greater than the pion-nucleon mass ratio, the hyperon recoil will almost certainly play an important part in K^+ meson photoproduction, even near threshold. Nevertheless, it is instructive to compare the experimental cross sections to those predicted by direct analogy to pion photoproduction.

It is a well-known fact that positive pion photoproduction exhibits s-wave behavior near threshold. The angular distribution is isotropic and there is a first-power dependence of the cross section on the momentum of the meson. There is, of course, a p-wave portion of the cross section characterized by a p^3 dependence and a $\sin^2\theta$ angular dependence. Since it is this portion of the cross section which is associated with the 3/2 - 3/2 resonance, it will not be considered

further. The s-wave term, however, leads to a direct evaluation of the meson-baryon coupling constant; it was, in fact, by this means that Bernardini and Goldwasser made the first reliable determination of the pion-nucleon coupling constant (25).

The Chew-theory formula for positive pion production near threshold is given by Gell-Mann and Watson (26) in a form which includes a modification to account for the nucleon recoil:

$$\left(\frac{d\sigma}{d\Omega}\right)_{CM} = \frac{1}{2M^2}\,\frac{e^2}{4\pi}\,\frac{G^2}{4\pi}\,\frac{p}{k}\left(1-\frac{E}{2M}\right)^2\left(1+\frac{k}{M}\right)^{-1}\left(1+\frac{E}{M}\right)^{-1} \qquad (12)$$

The meson C.M. energy is E; the meson C.M. momentum is p; the C.M. photon energy is k; and the nucleon mass is M. The term $G^2/4\pi$ is the renormalized pseudoscalar coupling constant. Units in which $\hbar = c = 1$ are used. The three terms enclosed in parenthesis form the recoil correction to the basic Chew-theory result; these terms are, in fact, small corrections in the pion case. If however, the K^+ meson is substituted for the pion, the recoil terms are greatly reduced, making a total correction of a factor five in the cross section. In this case, the recoil terms are probably not very accurate in accounting for the nuclear motion. However, in view of the desire to make a direct comparison of the experimental results to the predictions of pion theory, equation 12 is used in the following section to obtain a value for the K - Λ coupling constant and to make a comparison of the measured excitation function to the predicted one.

There is, of course, a certain reluctance to use simple perturbation theory for any calculation involving strongly interacting particles. Kroll and Ruderman (27) have shown, however, that for mesons of zero mass the perturbation calculations for meson photoproduction are exact if the coupling constant is renormalized. This has been shown to be correct in the case of pions near threshold; indeed, the Chew-theory result of equation 12 is just the perturbation theory result for a pseudoscalar meson. In the case of the K mesons, their mass is certainly quite different from zero, and the Kroll-Ruderman result might not be expected to be valid. Experimental evidence, however, points to the possibility that the coupling of K^+ mesons to baryons may be somewhat smaller than the pion-nucleon coupling constant, thus making perturbation theory more plausible.

Measurements on "strange" particle production in pion-nucleon collisions indicate a total cross section of approximately 1 millibarn (6). Serber (28) has analyzed the process on the basis of the Fermi statistical theory (29), which predicts a value for the cross section 5 times larger than that observed. "Strange" particle production in proton-proton collisions has also been studied, giving a total cross section of about 0.2 millibarn (7), also a factor of 5 smaller than the prediction of the statistical theory. In addition, the nuclear scattering of K^+ mesons, which has a cross section of about 10 millibarns, is considerably smaller than pion scattering. Stapp's Chew-type calculation (23) obtains a coupling constant which must be somewhat smaller than the pion-nucleon constant in order to fit the data. There

seems, therefore,to be a consistent set of evidence pointing to a smaller coupling of the K mesons than of the pions. Consequently, some reliance might be placed in the predictions of perturbation theory.

Moravcsik and Kawaguchi (30) and Fujii and Marshak (31) have made perturbation calculations assuming both scalar and pseudoscalar K mesons and assuming various values for the hyperon anomalous magnetic moments. The results predict a strikingly different behavior between the cross sections for scalar and pseudoscalar K mesons. They are compared to the results of this experiment in the following section.

Gell-Mann (32) has proposed a theory of the strong couplings in which pions are coupled universally to all baryons, which are degenerate in the absence of the K meson couplings. The K mesons are also coupled universally to the baryons, but with a weaker strength. The K mesons are then responsible for the separation of the baryons into the known hyperons and nucleons. The results of this experiment with regard to the K-Λ coupling constant are, as seen in the next section, consistent with the assumption of weaker K-coupling, as are the other experiments mentioned above. There are, unfortunately, no calculations based on Gell-Mann's theory as yet which pertain to K^+ meson photoproduction.

Christy (33) has proposed a model of the hyperons and K mesons in which a hyperon is regarded as a bound system containing a nucleon and an anti-K meson. The fundamental process in photoproduction in the virtual creation of a K-anti-K pair, the anti-K meson being then

bound to the nucleon, leaving the K meson free. Christy assumes a scalar interaction and uses the observed masses of the hyperons to fix certain of his parameters. If the interaction should actually be scalar, then K meson photoproduction should provide a critical test of his model, since his basic assumptions are not dependent on the photoproduction process.

VIII. INTERPRETATION OF RESULTS

In this section a comparison is made between the results of this experiment and the predictions of the theories discussed in the preceding section. The experimental results of other groups are also compared, where possible, to the results of this experiment. Because of the large statistical probable errors which must be assigned to the measured cross sections it is not possible to attach much significance to the agreement or disagreement of theory with experiment. Nevertheless, it is useful to make such comparisons in order to obtain a guide for the future study of K^+ meson photoproduction.

Since the direct pion analogy discussed in the preceding section (which is identical with pseudoscalar perturbation theory) should be close to an accurate description of the cross section if the K^+ meson is actually pseudoscalar, this is the first comparison made. It should be remembered that in this case the cross section is isotropic and proportional to the meson's C.M. momentum. Because of the expected isotropy the comparison is made to the 90 degree experimental points only. These are plotted in figure 15, the solid curve being a least-squares fit of the pseudoscalar perturbation calculation (30, 31) to the experimental points. The coupling constant obtained from this fit is $G^2/4\pi = 2.9 \pm 0.4$. The agreement is certainly quite good, but not necessarily significant. One point worth mention is that it seems likely that the cross section is appreciable for a photon energy only slightly above threshold. Measurements in the region between 910 Mev and 960 Mev would be of great importance in establishing the threshold

Figure 15. Excitation Function for the Reaction. $\gamma + P \rightarrow K^+ + \Lambda^0$.

This figure gives the measured cross sections at 90 degrees C.M.. The curves are least-squares fits of the perturbation calculations of Fujii and Marshak.

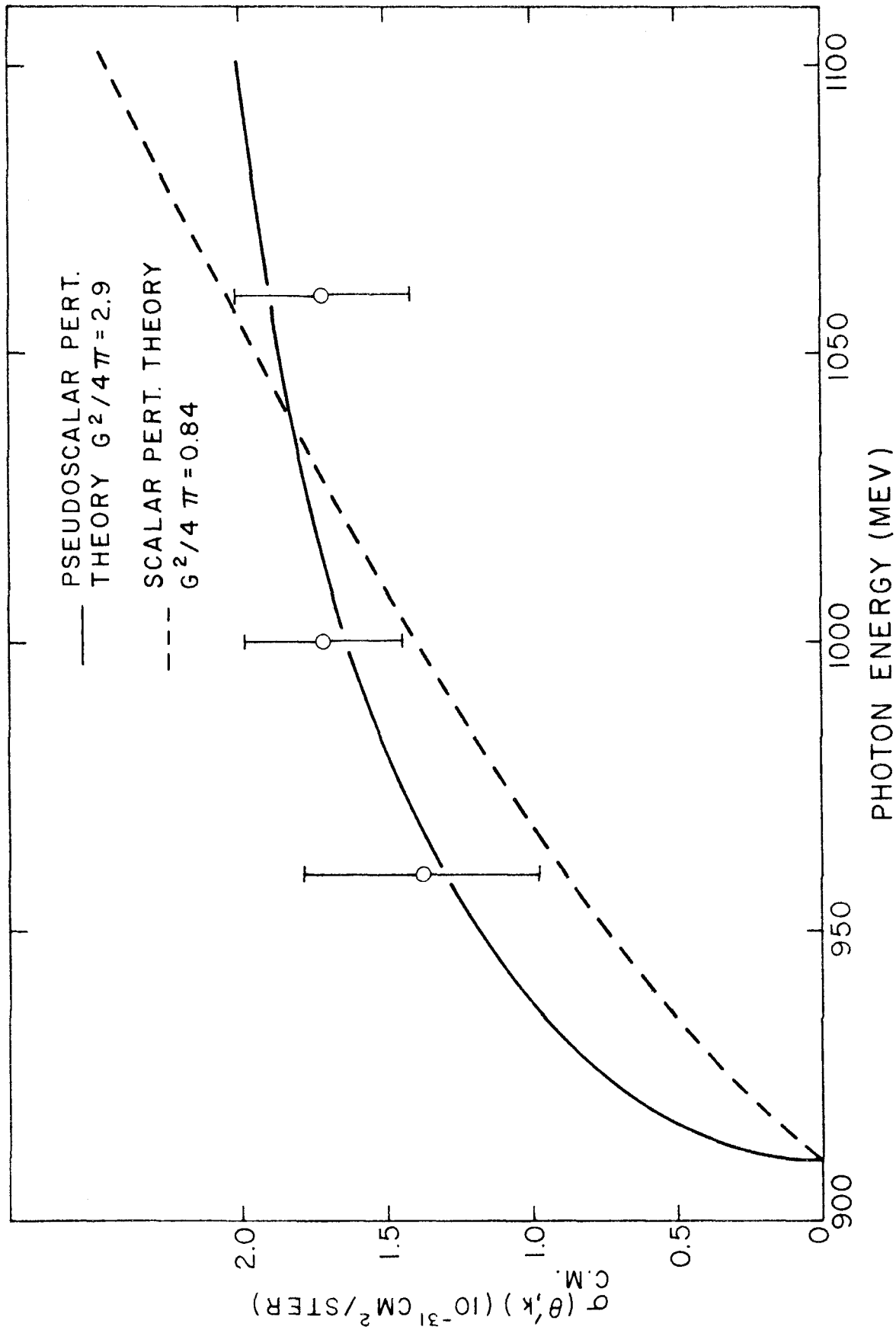
PSEUDOSCALAR PERT.
THEORY $G^2/4\pi = 2.9$
SCALAR PERT. THEORY
$G^2/4\pi = 0.84$
$\sigma_{c.m.}(\theta,k)$ $(10^{-31}$ CM^2/STER)
PHOTON ENERGY (MEV)
0
0.5
1.0
1.5
2.0
900
950
1000
1050
1100

momentum dependence of the cross section. The present data favor a first-power momentum dependence but do not, of course rule out a different behavior near threshold.

In figure 15 the scalar perturbation theory calculation (30, 31) is also compared to the experimental 90 degree points. A coupling constant of $G^2/4\pi = 0.84 \pm 0.14$ is required to make the fit. The agreement is certainly not so good as in the pseudoscalar case, but this is not surprising in view of the fact that the coupling constant required is quite large when used in a scalar theory. Despite the better agreement obtained in the pseudoscalar case, therefore, it is not possible to draw a definite conclusion about the parity of the K^+ meson.

When the scalar and pseudoscalar perturbation calculations are compared to the angular distributions at 1000 Mev, figure 16, and 1060 Mev, figure 17, the situation is exactly the opposite: the scalar fit is quite good, but not the pseudoscalar. The cross section reported by Wilson and Silverman (13) is included in figure 15. There seems to be a definite decrease in both angular distributions at backward angles. This is, however, consistent with both the scalar and the pseudoscalar perturbation calculations. Certainly more information on these angular distributions is needed, particularly at extremely forward and backward angles, where the scalar and pseudoscalar calculations differ.

Peterson, Roos, and Terman (11) have measured the cross section at a photon energy of 1030 Mev and a C.M. angle of 110 degrees. Their cross section is $2 \pm 0.8 \times 10^{-31}$ cm^2 per steradian, which agrees quite well with the values reported here. Ernstene, Gomez, Myers, and

Figure 16. Angular Distribution for the Reaction. $\gamma + P \rightarrow K^{+} + \Lambda^{o}$

This figure shows the measured points at 1000 Mev photon energy, and includes the measurement of Wilson and Silverman. The curves are least-squares fits of the perturbation calculations of Fujii and Marshak.

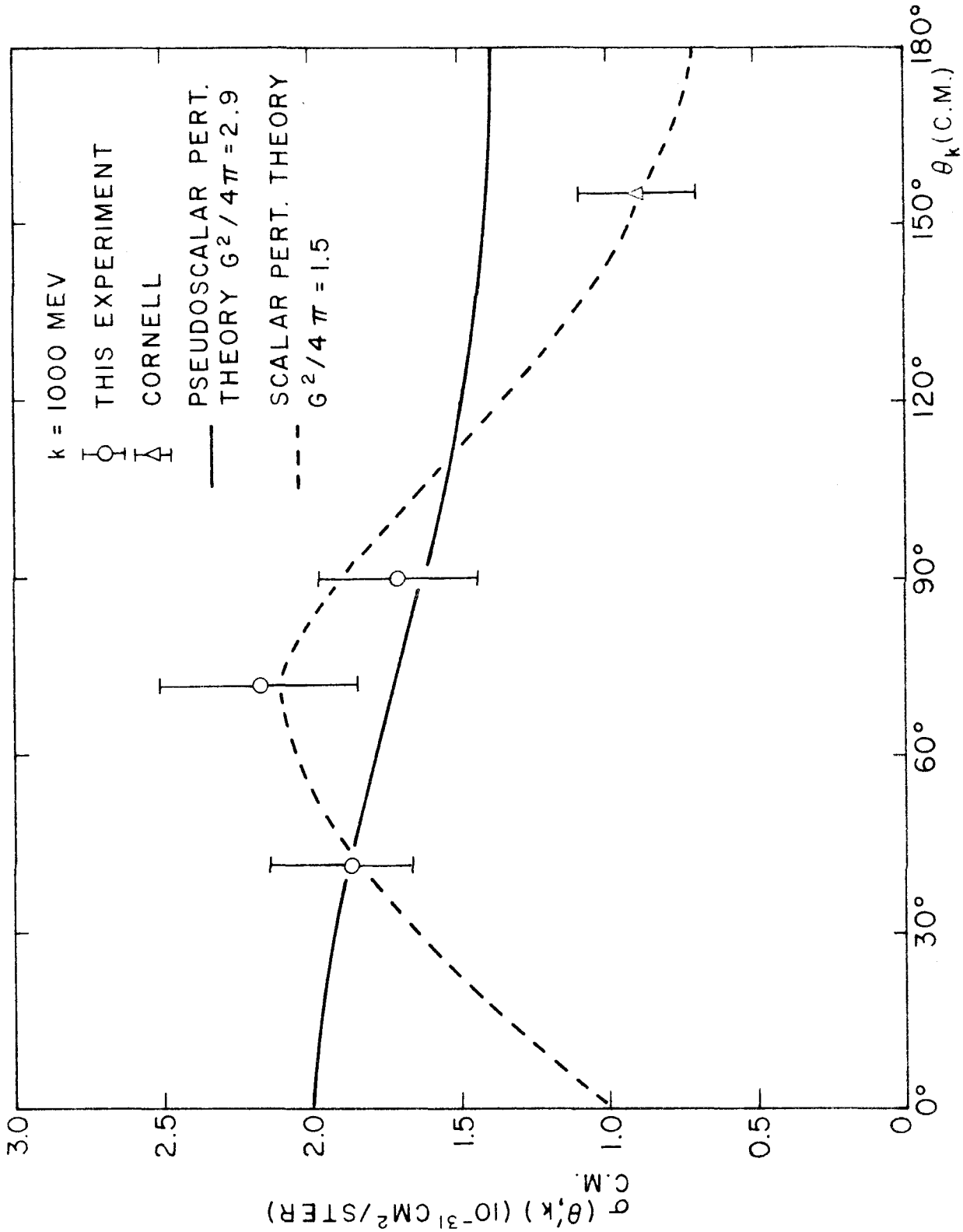
k = 1000 MEV
THIS EXPERIMENT
CORNELL
PSEUDOSCALAR PERT. THEORY $G^2/4\pi = 2.9$
SCALAR PERT. THEORY $G^2/4\pi = 1.5$
$\sigma_{c.m.}(\theta, k)$ (10^{-31} CM^2/STER)
θ_k (C.M.)
0
0.5
1.0
1.5
2.0
2.5
3.0
0°
30°
60°
90°
120°
150°
180°

Figure 17. Angular Distribution for the Reaction. $\gamma + p \rightarrow K^+ + \Lambda^0$

This figure gives the measured points at 1060 Mev photon energy. The curves are least-squares fits of the perturbation calculations of Fujii and Marshak.

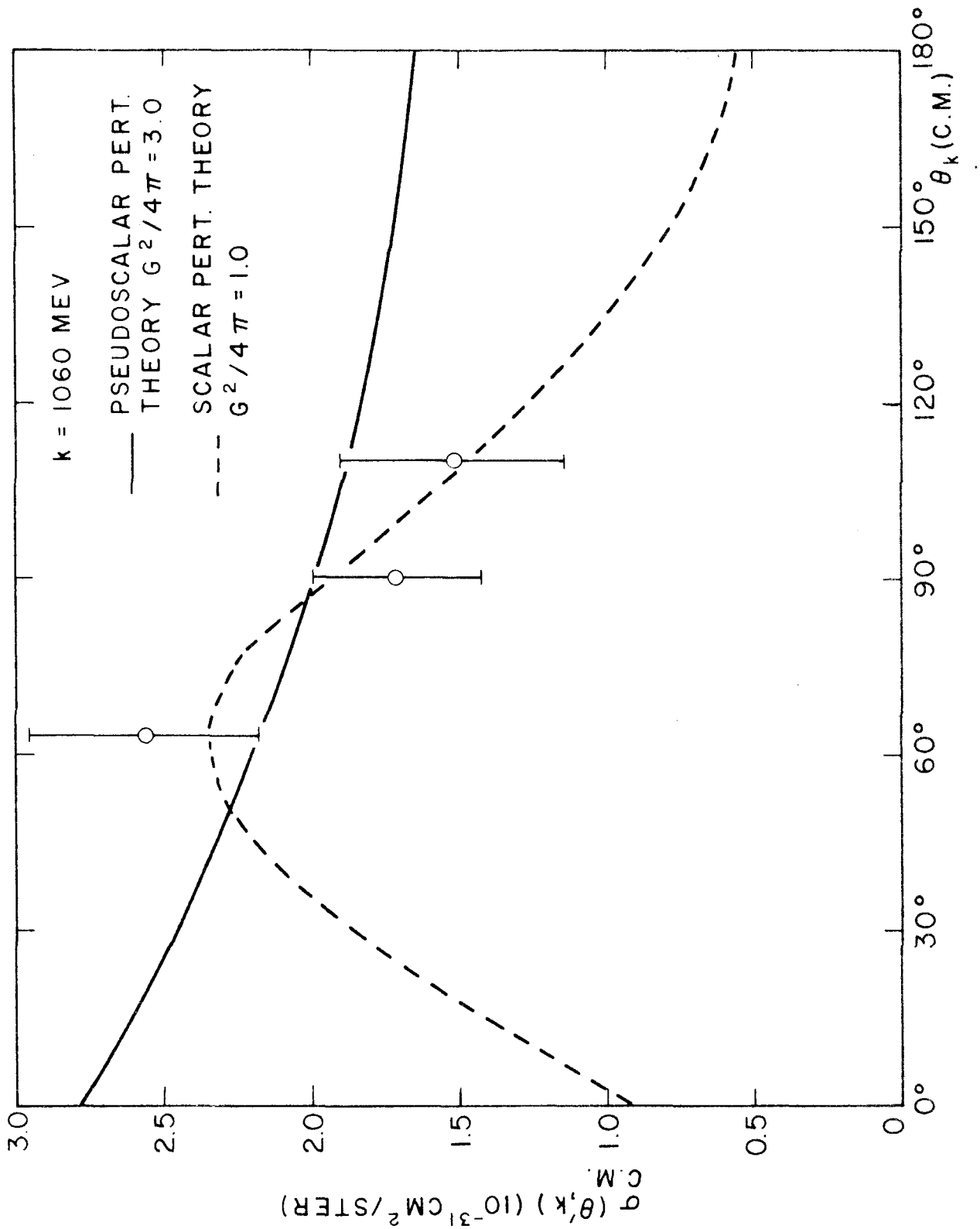
k = 1060 MEV
PSEUDOSCALAR PERT. THEORY $G^2/4\pi = 3.0$
SCALAR PERT. THEORY $G^2/4\pi = 1.0$
$\sigma_{c.m.}(\theta,k)$ (10^{-31} CM^2/STER)
θ_k(C.M.)
0
0.5
1.0
1.5
2.0
2.5
3.0
0°
30°
60°
90°
120°
150°
180°

Tollestrup (12) have made preliminary measurements which have not as yet yielded a number for the cross section.

IX. CONCLUSIONS

This experiment has established that K^+ mesons are produced in photon-nucleon collisions. It has further established that the K^+ mesons must be produced according to the law of associated production. This law is, therefore, valid, as expected, for electromagnetic processes.

With regard to the specific nature of the reaction

$$\gamma + P \rightarrow K^+ + \Lambda^o \qquad (1)$$

little can be said. The excitation function certainly shows s-wave behavior. P-wave behavior seems definitely ruled out on the basis of the excitation function, but is admissible on the basis of the angular distributions. More information is needed at photon energies very near threshold for the excitation function, and at extremely forward and backward angles for the angular distributions.

REFERENCES

1. M. Gell-Mann and A. Pais, Proceedings of the 1954 Glasgow Conference on Nuclear and Meson Physics, Pergamon, London (1955).

2. M. Gell-Mann, Phys. Rev., 92, 833 (1953).

3. T. Nakano and K. Nishijima, Prog. Theor. Phys., 10, 581 (1953).

4. M. Gell-Mann, Il Nuovo Cimento, IV, X, Supp., 2, 849 (1956).

5. L. W. Alvarez, Proceedings of the Seventh Rochester Conference, Interscience, New York (1957).

6. D. Glaser, Proceedings of the Seventh Rochester Conference, Interscience, New York (1957).

7. J. Orear, Proceedings of the Seventh Rochester Conference, Interscience, New York (1957).

8. J. Orear, Proceedings of the Seventh Rochester Conference, Interscience, New York (1957).

9. G. Puppi, Proceedings of the Seventh Rochester Conference, Interscience, New York (1957).

10. M. Perl, Proceedings of the Seventh Rochester Conference, Interscience, New York (1957).

11. V. Z. Peterson, C. E. Roos, and T. C. Terman, private communication.

12. M. P. Ernstene, R. Gomez, H. Myers, and A. V. Tollestrup, private communication.

13. R. R. Wilson and S. Silverman, preprint.

14. K. R. Symon, Thesis, Harvard University (1948).

15. P. L. Donoho, "A Magnetic Spectrometer for Analysis of Particles of Momentum Up to 1200 Mev/c", California Institute of Technology (1957), unpublished.

16. J. I. Vette and W. D. Wales, Low Energy Magnet Report, California Institute of Technology (1957), unpublished.

17. R. L. Walker, P. L. Donoho, and E. B. Emery, private communication.

18. R. Gomez, private communication.

19. R. R. Wilson, preprint.

20. D. D. Elliott, private communication.

21. R. L. Walker, private communication.

22. N. Dallaporta, Proceedings of the Seventh Rochester Conference, Interscience, New York (1957).

23. H. Stapp, Phys. Rev., 106, 134 (1957).

24. L. W. Alvarez, Proceedings of the Seventh Rochester Conference, Interscience, New York (1957).

25. G. Bernardini and E. L. Goldwasser, Phys. Rev., 95, 857 (1954).

26. M. Gell-Mann and K. M. Watson, Annual Reviews of Nuclear Science, 4, Annual Reviews, Stanford (1954).

27. N. M. Kroll and M. A. Ruderman, Phys. Rev., 93, 233 (1954).

28. R. Serber, Proceedings of the Seventh Rochester Conference, Interscience, New York (1957).

29. E. Fermi, Prog. Theor. Phys., 5, 570 (1950).

30. M. J. Moravcsik and M. Kawaguchi, Phys. Rev., 107, 563 (1957).

31. A. Fujii and R. E. Marshak, Phys. Rev., 107, 570 (1957).

32. M. Gell-Mann, Phys. Rev., 106, 1296 (1957).

33. R. F. Christy, Proceedings of the Seventh Rochester Conference, Interscience, New York (1957).